QUORUM SENSING AND HOST KILLING IN AN INSECT SYMBIOSIS

by

Abhishek Chari

A thesis submitted to the faculty of
The University of Utah
in partial fulfillment of the requirements for the degree of

Master of Science

Department of Biology

The University of Utah

May 2017

The University of Utah Graduate School

STATEMENT OF THESIS APPROVAL

The thesis of **Abhishek Chari**

has been approved by the following supervisory committee members:

Colin Dale	, Chair	**12/10/2015**
		Date Approved
David Blair	, Member	**12/10/2015**
		Date Approved
Jon Seger	, Member	**12/10/2015**
		Date Approved

and by **Denise Dearing** , Chair of

the Department of **Biology**

and by David B. Kieda, Dean of The Graduate School.

ABSTRACT

Sodalis praecaptivus is a recently isolated, novel bacterium that was isolated from a wound on the hand of a 71-year-old human patient. Phylogenetic analysis and comparative genomics revealed that this organism is closely related to members of the *Sodalis*-allied clade of insect endosymbiotic bacteria. This thesis deals with two investigations of this bacterium. The first is a study providing a physiological and biochemical characterization of this organism. The second is an analysis of the relationship between quorum sensing, virulence modulation against an insect host and a novel self-regulatory population control phenomenon in *S. praecaptivus*. It is proposed that using a population density signal to modulate virulence and growth could allow this organism to balance the need for host invasion against the need to maintain an asymptomatic infection of high density within an insect vector. This would allow the insect vector to transmit *S. praecaptivus* between potential plant and animal hosts without significant loss of fitness and might be a crucial step in the conversion of free living antecedent bacteria to mutualistic symbionts.

TABLE OF CONTENTS

LIST OF TABLES

LIST OF FIGURES

ACKNOWLEDGEMENTS

I would like to thank all the members of the Dale Lab, and the members of my committee for all their help and support during my time at the University of Utah.

1. INTRODUCTION

Bacteria that are obligately associated with their host are seen to have a reduced genome size and a reduced gene set that is compatible with the symbiotic lifestyle (1). The process of genome degeneration in obligate symbionts has been studied in great detail but the issue of how these obligate, mutualistic associations arose in the first place is still unresolved. Any organism that tries to colonize an insect must be able to do two things: evade or repel the host insect's immune response and be able to grow within the insect to maintain a continuous but asymptomatic infection. These two strategies will allow the bacteria to maintain the host or vector long enough to be able to transmit itself to other organisms that the vector comes into contact with (2). *Sodalis praecaptivus*, a novel bacterium isolated from a human patient, has been shown to be closely related to members of the Sodalis-allied clade of insect endosymbionts. This clade of endosymbiont bacteria is found in a wide range of insect hosts (3). Different mechanisms have been proposed for this spread of symbionts among such a wide range of insects, including the presence of environmental progenitor bacteria. Analyses comparing the genome sequences of *S. praecaptivus* and related insect symbionts highlight the possibility that close relatives of *S. praecaptivus* gave rise to mutualistic symbionts in a range of insect hosts (2). Chapter 1 focuses on the biochemical and phylogenetic analysis of *S. praecaptivus*, on the basis of which this organism was given formal scientific nomenclature. The tests shown in Chapter 1 also demonstrated that the organism has a wide repertoire of metabolic properties, which is consistent with the presence of a relatively large gene inventory (when compared to other members of the *Sodalis*-allied clade). *S. praecaptivus* was shown to be the first representative of the *Sodalis*-allied clade of bacteria that has sufficient metabolic capabilities to sustain growth in minimal media.

Chapter 2 focuses on the quorum sensing pathway that exists in *S. praecaptivus*. Mutants that lack either quorum signal synthesis or sensing ability were shown to kill grain

weevils that they were introduced into, in contrast to *S. praecaptivus* wild type bacteria that maintained an asymptomatic infection in them. *S. praecaptivus* was also shown to suppress its own growth under the influence of its quorum signal molecule. Taken together, these two chapters show the range of capabilities that *S. praecaptivus* has to exist.

It exists as a free-living organism while also being able to colonize an insect host without significantly affecting the host's fitness. It is hypothesized a commensal relationship between the bacterium and the insect would allow the insect to vector *S. praecaptivus* between potential animal and plant hosts. The ability of *S. praecaptivus* to not harm its host might also contribute to the widespread presence of the *Sodalis*-allied clade of bacteria in insects.

1.1 References

1. McCutcheon JP, von Dohlen CD. An interdependent metabolic patchwork in the nested symbiosis of mealybugs. Curr Biol. 2011;21(16):1366–72.

2. Clayton AL, Oakeson KF, Gutin M, Pontes A, Dunn DM, von Niederhausern AC, et al. A novel human-infection-derived bacterium provides insights into the evolutionary origins of mutualistic insect–bacterial symbioses. PLoS Genet. 2012;8(11):e1002990.

3. Snyder AK, McMillen CM, Wallenhorst P, Rio RV. The phylogeny of Sodalis-like symbionts are reconstrcuted using surface-encoding loci. FEMS Microbiol Lett. 2011;317(2):143-51.

2. PHENOTYPIC CHARACTERIZATION OF *SODALIS PRAECAPTIVUS* SP. NOV., A CLOSE NON-INSECT-ASSOCIATED MEMBER OF THE *SODALIS*-ALLIED LINEAGE OF INSECT ENDOSYMBIONTS

International Journal of Systematic and Evolutionary Microbiology (2015), **65**, 1400–1405 **DOI** 10.1099/ijs.0.000091

Phenotypic characterization of *Sodalis praecaptivus* sp. nov., a close non-insect-associated member of the *Sodalis*-allied lineage of insect endosymbionts

Abhishek Chari,[1] Kelly F. Oakeson,[1] Shinichiro Enomoto,[1] D. Grant Jackson,[1] Mark A. Fisher[2,3] and Colin Dale[1]

Correspondence
Abhishek Chari
abhishek.chari@utah.edu

[1]Department of Biology, University of Utah, 257 South 1400 East, Salt Lake City, UT 84112, USA

[2]Associated Regional and University Pathologists (ARUP) Institute for Clinical and Experimental Pathology, 500 Chipeta Way, Salt Lake City, UT, USA

[3]Department of Pathology, University of Utah School of Medicine, 15 North Medical Drive East, Salt Lake City, UT 84132, USA

A Gram-stain-negative bacterium, isolated from a human wound was previously found to share an unprecedentedly close relationship with *Sodalis glossinidius* and other members of the *Sodalis*-allied clade of insect symbionts. This relationship was inferred from sequence analysis of the 16S rRNA gene and genomic comparisons and suggested the strain belonged to a novel species. Biochemical and genetic analyses supported this suggestion and demonstrated that the organism has a wide repertoire of metabolic properties, which is consistent with the presence of a relatively large gene inventory. Among members of the *Sodalis*-allied clade, this is the first representative that has sufficient metabolic capabilities to sustain growth in minimal media. On the basis of the results of this study, we propose that this organism be classified as a representative of a novel species, *Sodalis praecaptivus* sp. nov. (type strain HS^T = DSM 27494^T = ATCC BAA-2554^T).

This study describes the physiological and biochemical characterization of a novel bacterium isolated from a human wound, previously described as 'strain HS' (Clayton *et al.*, 2012). Phylogenetic analysis and comparative genomics have revealed that this organism is closely related to members of the *Sodalis*-allied clade of insect endosymbiotic bacteria, representatives of which are found in a wide range of insect hosts (Chrudimský *et al.*, 2012; Clayton *et al.*, 2012; Snyder *et al.*, 2011) existing as both facultative and obligate mutualistic symbionts. The only exception to this rule is *Biostraticola tofi*, a basal representative of this clade that was isolated as part of a biofilm layer on a riverine limestone deposit (Verbarg *et al.*, 2008). Although strain HS^T was isolated from a hand wound in a human host, the original source of the wound was a dead tree branch, suggesting that strain HS^T is capable of persisting in or on both plant and animal tissues. In addition, the genome sequences of two closely related insect symbionts, *Sodalis glossinidius* and '*Candidatus* Sodalis pierantonius' SOPE (Oakeson *et al.*, 2014), were found to be subsets of the genome sequence of strain HS^T, suggesting that close relatives of strain HS may give rise to the *Sodalis*-allied insect symbionts in nature, possibly as a consequence of insects vectoring this bacterium between plant and animal hosts (Clayton *et al.*, 2012).

To date, all insect-associated members of this clade have been found to maintain degenerated gene inventories that contain large numbers of pseudogenes and mobile DNA (Belda *et al.*, 2010), or have substantially reduced genome size (McCutcheon & von Dohlen, 2011). Since the insect hosts provide a stable, highly nutritive and competition-free environment for the bacteria, relaxed selection leads to loss of bacterial genes that are not required to sustain the mutualistic relationship (Moran *et al.*, 2008). The degree of genome degeneration is therefore predicted to be proportional to the age/timespan of the insect–bacterial association. Since the *Sodalis*-allied clade of symbionts contains representatives with relatively large (e.g. *Sodalis glossinidius*, '*Candidatus* Sodalis melophagi') (Chrudimský *et al.*, 2012) and small (e.g. *Wigglesworthia glossinidia*) genome sizes, it appears to include symbionts that are

The GenBank/EMBL/DDBJ accession numbers for the draft genome of strain HS^T are CP006569.1 (chromosome) and CP006570.1 (plasmid), those for the 16S rRNA and *groEL* gene are JX444565 and JX444566, respectively.

A supplementary list, one supplementary figure and one supplementary table are available with the online Supplementary Material.

both recent and ancient in origin (Moran *et al.*, 2008). As might be expected, genome degeneration makes it difficult to culture insect symbionts in the laboratory because they become increasingly fastidious over time (Pontes & Dale, 2006). To date, only two members of the *Sodalis*-allied clade, *Sodalis glossinidius* and '*Candidatus* Sodalis melophagi' have been successfully cultured *in vitro* and notably, they can only be grown in rich media (Chrudimský *et al.*, 2012; Dale & Maudlin, 1999).

Whole genome sequencing demonstrated that strain HS^T possesses a relatively large genome, of 5.16 Mb (Clayton *et al.*, 2012). It lacks any signs of the genome degradation that is apparent in insect-associated relatives (Clayton *et al.*, 2012). This suggests that strain HS has a larger set of metabolic capabilities, including the capability to utilize a wider range of carbon and nitrogen sources. The current study shows that, compared with *Sodalis glossinidius*, strain HS^T does indeed possess more extensive metabolic capability and can grow in defined, minimal media with only a carbon source, nitrogen source and salts. Strain HS^T is also capable of utilizing carbon sources found in plants as well as animals. In this work we compare the biochemical properties of strain HS^T with a number of animal and plant pathogens, and close relatives including *B. tofi* and *Sodalis glossinidius*. We describe phenotypic characteristics that will allow researchers to identify strain HS^T in the environment. On the basis of results of the current study and comparative genome sequence analysis (Clayton *et al.* 2012), the name *Sodalis praecaptivus* sp. nov. is proposed to accommodate strain HS^T.

Strain HS^T was isolated from serous fluid collected from a wound on the hand of a 71-year-old human patient. The patient's hand was impaled with a branch from a dead crab apple tree. The organism was isolated on MacConkey agar plates and grown at 35°C, under an atmosphere of 5% CO_2. The subsequent clinical course of treatment and aspiration of fluid from the wound were described previously (Clayton *et al.*, 2012). Strain HS^T was able to grow on M9 minimal agar media (List S1, available in the online Supplementary Material), at 30 and 37°C, in an ambient atmosphere. Two variants of M9 media with different nitrogen sources (ammonium chloride and sodium nitrate) were utilized.

Unlike *Sodalis glossinidius* (Dale & Maudlin, 1999) and '*Candidatus* Sodalis melophagi' (Chrudimský *et al.*, 2012), strain HS^T is capable of growth in minimal media. The organism grew equally well on both types of M9 agar media, indicating the ability to utilize both ammonia and nitrate as nitrogen sources.

Phylogenetic analysis was performed using 16S rRNA gene and *groEL* sequences obtained during the sequencing of the *Sodalis praecaptivus* sp. nov. draft genome (Clayton *et al.*, 2012). These were aligned with 16S rRNA gene and *groEL* nucleotide sequences obtained from the GenBank database for a range of endosymbiotic and free-living Gram-stain-negative bacteria (Fig. 1a, b). Sequence alignments were generated using MUSCLE (Edgar, 2004) and PhyML (Guindon & Gascuel, 2003) and used to reconstruct phylogenetic trees using the HKY85 (Hasegawa *et al.*, 1985) model of sequence evolution with 25 random starting trees and 100 bootstrap replicates. In accordance with previous findings (Clayton *et al.*, 2012), the phylogenetic analysis based on 16S rRNA and *groEL* gene sequences placed strain HS^T in a clade with high bootstrap support with members of the *Sodalis*-allied insect symbionts (Fig. 1a, b). On the basis of 16S rRNA gene sequence analysis, the relationship between *B. tofi* and its most closely related insect endosymbiont (*Sodalis glossinidius*; 96.5 % sequence identity) is substantially more distant than that of strain HS^T and its closest insect-associated relative ('*Candidatus* Sodalis pierantonius' SOPE; >99 % sequence identity). The placement of *B. tofi* on a relatively long branch corroborates this finding and stands in contrast to the placement of strain HS^T on a very short branch, indicating that *B. tofi* is more distantly related and that strain HS^T is more likely to have served as an evolutionary precursor of the *Sodalis*-allied insect symbionts; a proto-symbiont, as proposed previously (Clayton *et al.*, 2012). In comparison with insect-associated members of this clade, Strain HS^T displays a relatively low rate of evolution of its 16S rRNA gene sequence. Other slow-evolving lineages are the symbionts of stinkbugs (*Cantao ocellatus*) and chestnut weevils (*Curculio sikkimensis*), which are predicted to have a recent origin in terms of their insect association (Kaiwa *et al.*, 2010; Toju & Fukatsu, 2011; Toju *et al.*, 2010). Notably, symbionts with small genome sizes, which are predicted to have a more ancient symbiotic origin, such as *W. glossinidia* and species of the genus *Blochmannia*, are localized on the longest branches in the tree. This is compatible with the notion that these bacteria are more ancient derivatives of a strain HS^T-like ancestor that have been subject to longer periods of accelerated sequence evolution in their insect hosts. However, we cannot exclude the possibility that the placement of these sequences in the *Sodalis*-allied clade is a consequence of long-branch attraction in the phylogenetic analysis.

The DNA G+C content of strain HS^T was extracted from the draft genome sequence and found to be 57.5 %.

MALDI-TOF (matrix assisted laser desorption ionization – time of flight) MS fingerprinting was performed on strain HS^T and *Sodalis glossinidius* essentially as previously described for identification of clinical isolates (Khot *et al.*, 2012). Bacterial cells (~5 to 10 mg) were obtained from duplicate cultures on MM blood agar media (media composition in List S1) for *Sodalis glossinidius* and strain HS^T or directly extracted from insect host tissue (for the symbionts of grain weevils *Sitophilus oryzae* and *Sitophilus zeamais*), and suspended in 300 µl distilled water and mixed by inversion with 900 µl absolute ethyl alcohol. Cells were pelleted (16 000 *g*, 2 min), and the supernatant was discarded followed by a second centrifugation (16 000 *g*, 2 min) and aspiration of any remaining ethanol. Cells were resuspended in 50 µl 70 % formic

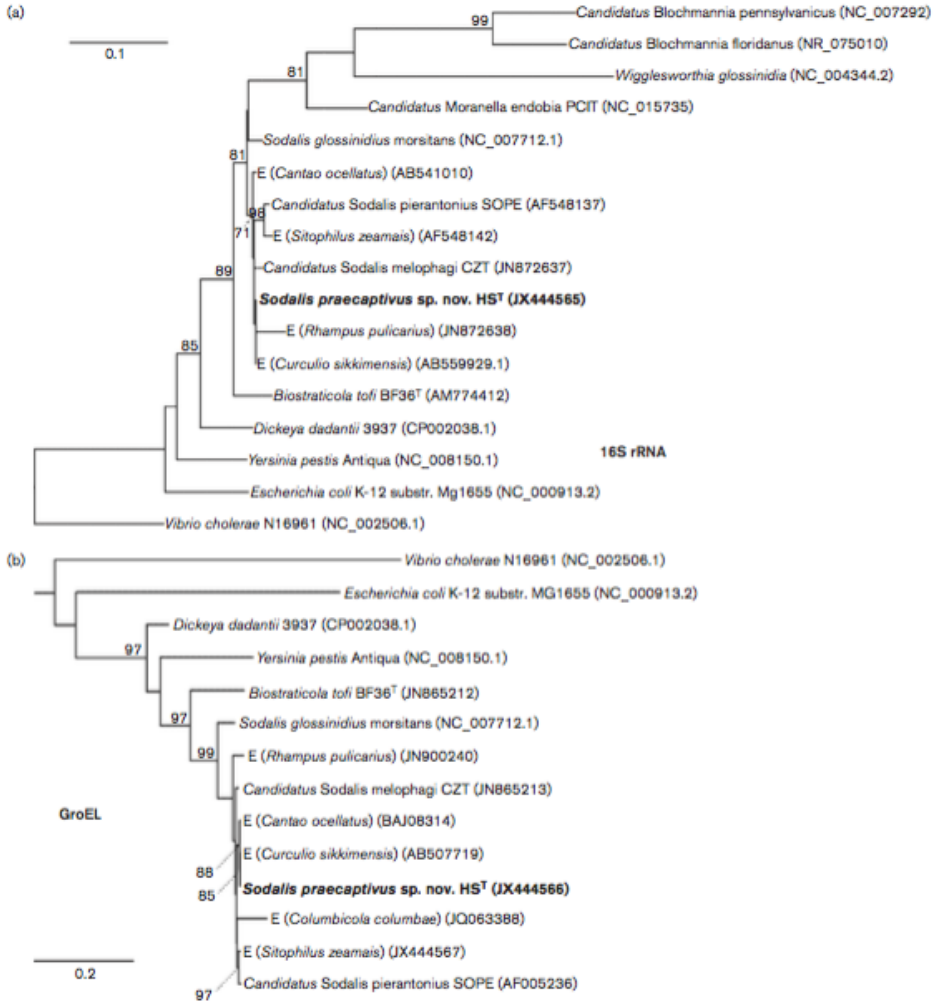

Fig. 1. Phylogeny of strain HS^T and related *Sodalis*-allied endosymbionts and free-living bacteria based on maximum-likelihood analyses of 16S rRNA (Fig. 1a) and *groEL* (Fig. 1b) nucleotide sequences. Insect endosymbionts that do not have formal nomenclature are designed by the prefix 'E', followed by the name of their insect host. Numbers adjacent to nodes indicate maximum-likelihood bootstrap values shown for nodes with bootstrap support greater than 70 %. Bars, 0.1 (a) or 0.2 (b) substitutions per site.

acid, vortexed for 1 min and mixed by pipetting with 50 µl pure acetonitrile. Samples were centrifuged (16 000 *g*, 2 min), and 75 µl of supernatant (bacterial extract) was transferred to fresh tubes. Bacterial extract (1 µl) from each replicate culture was spotted in triplicate onto polished steel targets, air-dried and overlaid with 1 µl

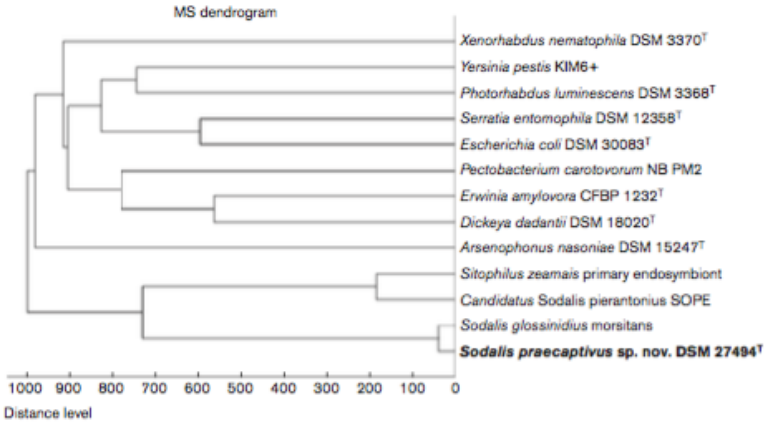

Fig. 2. MALDI-TOF MS dendrogram, derived from comparison of the *Sodalis praecaptivus* sp. nov. profile with those of *Sodalis glossinidius*, *Sitophilus oryzae* primary endosymbiont ('*Candidatus* Sodalis pierantonius' SOPE), *Sitophilus zeamais* primary endosymbiont and selected reference strains from the Bruker Daltonics Biotyper v 4.0.0.1 database. The distance level is normalized to a maximum value of 1000.

HCCA matrix, which was allowed to air dry. Mass spectra were acquired, for generation of custom MS spectra with a total of 24 replicate sum spectra for each isolate, between 2000 and 20 000 *m/z* in linear positive ionization mode (Microflex, Bruker Daltonics). MS profiles and MSP dendrograms were created with Biotyper 3.1 software (Database version 4.0.0.1, 5627 MS profiles, Bruker Daltonics) using the manufacturer's recommended settings. The MALDI-TOF MS dendrogram analysis was supportive of the phylogenetic analysis, showing that strain HS^T grouped together with *Sodalis glossinidius* and the closely related symbionts from the grain weevils, *Sitophilus zeamais* and *Sitophilus oryzae* (Fig. 2), which were placed in a clade separate from other members of the family *Enterobacteriaceae*, including the phylogentically distinct insect symbiont *Arsenophonus nasoniae*. It is of interest to note that the MALDI-TOF analysis of the grain weevil symbionts was performed on bacterial cells isolated directly from insect tissues, highlighting the utility of this method for the identification of symbionts *in vivo*. Furthermore, the addition of the current MS data to the Bruker Biotyper database should facilitate identification of relatives of strain HS^T in future clinical and environmental samples, potentially furthering our understanding of the ecology of these bacteria.

Biochemical characterization and substrate utilization tests were performed using the API 20E and API 50CH systems (bioMérieux), according to manufacturer's recommendations, to assess enzyme activity and fermentation/utilization of carbon sources. Catalase activity was determined using 3 % (v/v) H_2O_2 and chitinase activity was determined using a fluorimetric assay, CS 1030 (Sigma-Aldrich), according to the manufacturer's recommendations. Since previously characterized members of the *Sodalis*-allied clade of endosymbionts are metabolically dependent on their hosts, phenotypic tests have only been performed on *Sodalis glossinidius*, which has been obtained in pure culture (Dale & Maudlin, 1999). Owing to this fact, the *Sodalis*-allied clade is largely not amenable to phenotypic testing. Comparison of carbon source utilization traits showed that strain HS^T can be distinguished by at least three phenotypic characteristics from its closest relatives, *Sodalis glossinidius* and *B. tofi* (Table 1). Notably, strain HS^T could utilize sugars that are plant-based (e.g. cellobiose, xylose, rhamnose) and animal-based (e.g. lactose). In addition, strain HS^T could grow at 37°C whereas *B. tofi* and *Sodalis glossinidius* are incapable of growth at temperatures exceeding 30°C (Verbarg *et al.*, 2008; Dale & Maudlin 1999). It is interesting to note that strain HS^T can utilize melezitose and trehalose, sugars that are predominantly found in aphids and insects, respectively (Owen, 1978; Elbein *et al.*, 2003). This coupled with the fact that strain HS^T can produce chitinase as well as utilize *N*-acetylglucosamine, a building block of insect exoskeleton polymer chitin (Merzendorfer & Zimoch, 2003), indicates that strain HS^T has the metabolic potential to derive nutrition from an insect source. Notably, *Sodalis*-allied symbionts are found in a wide range of insect hosts, known to feed either on animals (e.g. blood-feeding tsetse flies) or plants (e.g sap-feeding psyllids), which is consistent with the

Table 1. Comparison of carbon source fermentation

Species: 1, *Sodalis praecaptivus* sp. nov.; 2, *Biostraticola tofi* (Verbarg *et al.*, 2008); 3, *Sodalis glossinidius* (Dale & Maudlin, 1999). +, Positive; W, weakly positive; −, negative; V, variable; ND, not determined. None of the species could ferment maltose or salicin.

Carbon source	1	2	3
D-Lyxose	+	ND	ND
D-Mannose	+	+	−
L-Rhamnose	+	+	−
D-Xylose	+	+	−
L-Arabinose	+	+	−
Lactose	+	+	−
Glycerol	W	+	−
D-Sorbitol	+	−	+
Cellobiose	W	+	ND
Melibiose	+	−	−
D-Tagatose	+	ND	ND
Arbutin	−	+	ND

notion that close relatives of strain HS^T have given rise to symbionts in both animal and plant-feeding insects.

As detailed above, unlike the insect-associated relatives of *Sodalis glossinidius*, strain HS^T is capable of growth on minimal media, consistent with its free-living/opportunistic lifestyle. Thus, for its formal nomenclature, selection of the species epithet (*praecaptivus*) was based on the inference that strain HS^T is a free-living environmental precursor of the *Sodalis*-allied clade of insect symbionts.

Description of *Sodalis praecaptivus* sp. nov.

Sodalis praecaptivus (prae.cap.ti'vus, L. prep. *prae* before; L. masc. adj. *captivus* taken prisoner; N.L. masc. adj. *praecaptivus* not yet taken prisoner).

Cells are aerobic, Gram-stain-negative, non-spore-forming short rods (2 µm in length, 1–1.5 µm in diameter). The colonies are white, rounded, mucoid and 1–2 mm in diameter after 24 h of growth at 30°C on LB agar plates. Growth is observed on LB agar, MacConkey agar, Columbia blood agar, MM blood agar and M9 agar from 25°C to 37°C. Exhibits swarming motility on LB agar (Fig. S1) and grows in LB broth at an optimal pH of 5.5 and a maximum NaCl concentration of 3.5 %. Utilizes the following carbon sources: glycerol, D-arabinose, L-arabinose, D-ribose, D-xylose, D-galactose, D-glucose, D-fructose, D-mannose, L-rhamnose, inositol, D-mannitol, D-sorbitol, methyl α-D-glucopyranoside, *N*-acetylglucosamine, amygdalin, aesculin ferric citrate, cellobiose, lactose, melibiose, sucrose, trehalose, raffinose, melezitose, inulin, starch, glycogen, xylitol, gentiobiose, turanose, D-lyxose, D-tagatose, D-fucose, L-fucose, D-arabitol, potassium gluconate and potassium-5-ketogluconate. Produces catalase, chitinase and β-galactosidase. Carbon source utilization test results are tabulated in Table S1.

The type strain is HS^T (= DSM 27494^T = ATCC BAA-2554^T), isolated from a human patient in the USA. The genomic G+C content of the type strain is 57.5 %.

Acknowledgements

This research was supported by National Institutes of Health (www.nih.gov) grant 1R01AI095736 (to C. D.) and the ARUP Institute for Clinical and Experimental Pathology (M. A. F.).

References

Belda, E., Moya, A., Bentley, S. & Silva, F. J. (2010). Mobile genetic element proliferation and gene inactivation impact over the genome structure and metabolic capabilities of *Sodalis glossinidius*, the secondary endosymbiont of tsetse flies. *BMC Genomics* **11**, 449.

Chrudimský, T., Husník, F., Nováková, E. & Hypša, V. (2012). *Candidatus* Sodalis melophagi sp. nov.: phylogenetically independent comparative model to the tsetse fly symbiont *Sodalis glossinidius*. *PLoS ONE* **7**, e40354.

Clayton, A. L., Oakeson, K. F., Gutin, M., Pontes, A., Dunn, D. M., von Niederhausern, A. C., Weiss, R. B., Fisher, M. & Dale, C. (2012). A novel human-infection-derived bacterium provides insights into the evolutionary origins of mutualistic insect-bacterial symbioses. *PLoS Genet* **8**, e1002990.

Dale, C. & Maudlin, I. (1999). *Sodalis* gen. nov. and *Sodalis glossinidius* sp. nov., a microaerophilic secondary endosymbiont of the tsetse fly *Glossina morsitans morsitans*. *Int J Syst Bacteriol* **49**, 267–275.

Edgar, R. C. (2004). MUSCLE: multiple sequence alignment with high accuracy and high throughput. *Nucleic Acids Res* **32**, 1792–1797.

Elbein, A. D., Pan, Y. T., Pastuszak, I. & Carroll, D. (2003). New insights on trehalose: a multifunctional molecule. *Glycobiology* **13**, 17R–27R.

Guindon, S. & Gascuel, O. (2003). A simple, fast, and accurate algorithm to estimate large phylogenies by maximum likelihood. *Syst Biol* **52**, 696–704.

Hasegawa, M., Kishino, H. & Yano, T. (1985). Dating of the human-ape splitting by a molecular clock of mitochondrial DNA. *J Mol Evol* **22**, 160–174.

Kaiwa, N., Hosokawa, T., Kikuchi, Y., Nikoh, N., Meng, X. Y., Kimura, N., Ito, M. & Fukatsu, T. (2010). Primary gut symbiont and secondary, *Sodalis*-allied symbiont of the Scutellerid stinkbug *Cantao ocellatus*. *Appl Environ Microbiol* **76**, 3486–3494.

Khot, P. D., Couturier, M. R., Wilson, A., Croft, A. & Fisher, M. A. (2012). Optimization of matrix-assisted laser desorption ionization-time of flight mass spectrometry analysis for bacterial identification. *J Clin Microbiol* **50**, 3845–3852.

McCutcheon, J. P. & von Dohlen, C. D. (2011). An interdependent metabolic patchwork in the nested symbiosis of mealybugs. *Curr Biol* **21**, 1366–1372.

Merzendorfer, H. & Zimoch, L. (2003). Chitin metabolism in insects: structure, function and regulation of chitin synthases and chitinases. *J Exp Biol* **206**, 4393–4412.

Moran, N. A., McCutcheon, J. P. & Nakabachi, A. (2008). Genomics and evolution of heritable bacterial symbionts. *Annu Rev Genet* **42**, 165–190.

Oakeson, K. F., Gil, R., Clayton, A. L., Dunn, D. M., von Niederhausern, A. C., Hamil, C., Aoyagi, A., Duval, B., Baca, A. & other authors (2014). Genome degeneration and adaptation in a nascent stage of symbiosis. *Genome Biol Evol* **6**, 76–93.

Owen, D. F. (1978). Why do aphids synthesize melezitose? *Oikos* **31**, 264–267.

Pontes, M. H. & Dale, C. (2006). Culture and manipulation of insect facultative symbionts. *Trends Microbiol* **14**, 406–412.

Snyder, A. K., McMillen, C. M., Wallenhorst, P. & Rio, R. V. (2011). The phylogeny of *Sodalis*-like symbionts as reconstructed using surface-encoding loci. *FEMS Microbiol Lett* **317**, 143–151.

Toju, H. & Fukatsu, T. (2011). Diversity and infection prevalence of endosymbionts in natural populations of the chestnut weevil: relevance of local climate and host plants. *Mol Ecol* **20**, 853–868.

Toju, H., Hosokawa, T., Koga, R., Nikoh, N., Meng, X. Y., Kimura, N. & Fukatsu, T. (2010). "*Candidatus* Curculioniphilus buchneri," a novel clade of bacterial endocellular symbionts from weevils of the genus *Curculio*. *Appl Environ Microbiol* **76**, 275–282.

Verbarg, S., Frühling, A., Cousin, S., Brambilla, E., Gronow, S., Lünsdorf, H. & Stackebrandt, E. (2008). *Biostraticola tofi* gen. nov., spec. nov., a novel member of the family *Enterobacteriaceae*. *Curr Microbiol* **56**, 603–608.

SUPPLEMENTARY SECTION

Table S1: API 50 CH assay

Molecule	ferm. in HS (30°C)	ferm. in (HS 35°C)	fermented by HS
Glycerol	Y	Y	+
Erythritol	N	N	-
D-arabinose	Y	Y	+
L-arabinose	Y	Y	+
D-ribose	Y	Y	+
D-xylose	Y	Y	+
L-xylose	N	N	-
D-adonitol	N	N	-
Methyl β D xylopyranoside	N	N	-
D-galactose	Y	Y	+
D-glucose	Y	Y	+
D-fructose	Y	Y	+
D-mannose	Y	Y	+
L-sorbose	N	N	-
L-rhamnose	Y	Y	+
Dulcitol	N	N	-
Inositol	N	Weak	+
D-mannitol	Y	Y	+
D-sorbitol	Y	Y	+
Methyl α D mannopyranoside	N	N	-
Methyl α D glucopyranoside	N	Weak	+
N-acetyl glucosamine	Y	Y	+
Amygdalin	N	Weak	+
Arbutin	N	N	-
Esculin ferric citrate	Weak	Weak	+
Salicin	N	N	-
D-cellobiose	Weak	Weak	+
D-maltose	N	N	-
D-lactose	Y	Y	+
D-melibiose	Y	Y	+
D-saccharose	N	Weak	+
D-trehalose	Y	Y	+
Inulin	N	Weak	+

D-melezitose	Weak	Weak	+
D-raffinose	Weak	Weak	+
Starch	Weak	N	+
Glycogen	Weak	N	+
Xylitol	Y	Y	+
Gentiobiose	N	Weak	+
D-turanose	Weak	Weak	+
D-lyxose	Y	Y	+
D-tagatose	Y	Y	+
D-fucose	Weak	Weak	+
L-fucose	Y	Weak	+
D-arabitol	Weak	Weak	+
L-arabitol	N	N	-
Potassium gluconate	Y	Y	+
2-Keto gluconate	N	N	-
5-Keto gluconate	Y	Y	+

(ferm.) fermented, (Y) positive fermentation, (N) no fermentation, (Weak) observed weak fermentation, (+) fermentable, (-) non-fermentable

List S1: M9 Media

Prepare 5X M9 salts solution: Changing **nitrogen source** for media variants (64 gm $Na_2HPO_4.7H_2O$, 15 gm KH_2PO_4, 2.5 gm NaCl, 5 gm **NH_4Cl or** 7.94 gm **$NaNO_3$** – dissolve these in, and make up total volume to 1000 ml, using ddH_2O and filter sterilize.)

For working media of 1X M9 (1 litre);

Add 15 gm of agar to ~780 ml distilled water (autoclave for 30 minutes)

Cool down agar solution to 52°C, mix agar solution with 200 ml aliquot of 5X M9 salts solution already maintained at 52°C, then add the following:

2 ml of 1 M $MgSO_4$ solution

0.1 ml of 1M $CaCl_2$ solution

20 ml of 20 % glucose

Swirl to mix and pour to make plates.

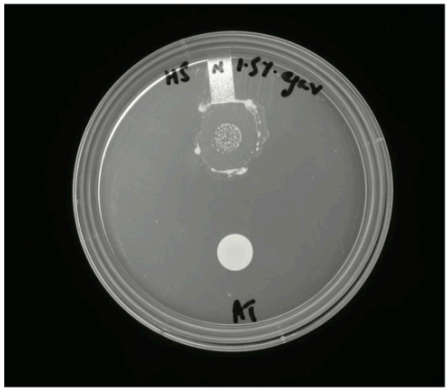

Figure S1: **Swarming motility** of *Sodalis praecaptivus* sp. nov. (designated 'HS' on the plate) on 1.5% LB agar plate. Comparison with non-motile *Agrobacterium tumefaciens* KYC55 (designated 'AT' on the plate. Overnight cultures of both organisms were spotted (25 µl) onto the plate and the image captured after 48 hrs incubation at room temperature.

3. AN INSECT KILLING PHENOTYPE IN *SODALIS PRAECAPTIVUS* QUORUM SENSING MUTATIONS

AUTHORS: Shinichiro Enomoto[a], Abhishek Chari[a], Adam.L.Clayton[a], Colin Dale[a]

[a] Department of Biology, University of Utah, 257 South 1400 East, Salt Lake City, UT 84112, USA.

3.1 Abstract

Many bacteria utilize quorum sensing (QS) to mediate control of gene expression in accordance with changes in their cell population density. This affects many important biological processes including the activation of virulence factors that bacteria utilize to effect disease. In the current study, we analyzed the functions of a QS system found in *Sodalis praecaptivus*, which is a close relative and putative environmental progenitor of the insect-associated *Sodalis*-allied symbionts, some of which maintain homologous QS systems. Our work shows that mutant strains of *S. praecaptivus*, lacking critical components of the QS machinery, have a rapid and potent killing phenotype following microinjection into an insect host. Transcriptomic and genetic analyses indicate that insect killing occurs as a consequence of virulence factors, including insecticidal proteins, whose expression is normally suppressed at high cell density by the QS regulatory circuit. Although the mechanistic functions of QS are similar between *S. praecaptivus* and a derived symbiotic relative, *S. glossinidius*, genes encoding insecticidal proteins have been lost in the transition to mutualistic associations in the *Sodalis*-allied symbionts. We discuss the implications of the unusual functionality of this QS system in the context of the origin and evolution of mutualistic relationships involving these bacteria.

3.2 Introduction

The regulation of gene expression is an important adaptive trait that allows organisms to modulate their physiology in response to changes in their environment. One such mechanism of regulation in bacteria involves a process known as quorum sensing (QS), in which bacteria synthesize an autoinducer signal (pheromone) that increases in concentration in accordance with bacterial population density (1,2). Using specific transcriptional regulators, bacteria then respond to specific threshold concentrations of the autoinducer in their environment and modulate gene expression accordingly (2).

The process of QS is a common method of modulating behavior and physiology in a wide range of bacteria, including pathogens (3). By pairing the expression of many virulence genes with bacterial population density, pathogens can mount an intense attack on their host when their

population density reaches a sufficient level to overcome host defenses (4). For example, *S. aureus* produces exotoxins and tissue-degrading enzymes at the end of its exponential growth phase (5). Similarly, the secretion of exoenzymes contributing to the plant pathogenicity of *E. carotovora* occurs in a growth phase dependent manner (6,7).

However, QS is also known to facilitate mutualistic interactions. For example, in the squid-*Vibrio fisheri* symbiosis, QS controls the expression of bacterial bioluminescence in the squid light organ, preventing the host from casting a shadow under the moonlit night sky and attracting predators (8,9). Working in concert with a daily cycle of symbiont expulsion and regrowth, this ensures that *V. fischeri* only achieves a bioluminescent quorum during the hours of darkness (Boettcher, Ruby, and McFall-Ngai 1996; K.-H. Lee and Ruby 1994; Ruby and Asato 1993).

In a previous study, we discovered a QS system in the tsetse fly symbiont, *Sodalis glossinidius*. Microarray analyses showed that the system controlled genes involved in the oxidative stress response, but we were unable to generate a QS-deficient mutant strain of this symbiont to determine the role of its QS system *in vivo* (13). In the current study, we have focused on a relative of *S. glossinidius*, known as *S. praecaptivus*, which was recently discovered in a human hand wound (14). Close relatives of *S. praecaptivus* have been found in a wide range of insect hosts such as cerambycid beetles (15), archaeococcoid scale insects (16), bird lice (17), spittlebugs (18), potato psyllids (19), mealybugs (20) and louse flies (21,22). In many cases, these bacteria are known to provide beneficial functions for their insect host (23). Comparative genomic analyses indicate that these mutualistic symbionts evolved repeatedly and independently from an *S. praecaptivus*-like ancestor, undergoing genome degeneration and size reduction as a consequence of the loss of genes that lack adaptive value following the transition to symbiosis (14). In addition, very close relatives of *S. praecaptivus* have been identified in a range of stinkbugs (24–26), where they seem to exist as transient (i.e. non-maternally transmitted) associates (27), consistent with the notion that their insect hosts serve as vectors for the transmission of these bacteria between plant hosts (14).

Since *S. praecaptivus* is readily amenable to laboratory manipulation, it serves as a

platform to investigate the functions of genes that are retained in closely related insect symbionts that are refractory to laboratory culture and/or genetic manipulation. In addition, this approach can yield valuable insight into the nature of the establishment of symbiotic relationships, especially given the fact that the *Sodalis*-allied symbionts seem to be particularly predisposed to evolving mutualistic associations with insects.

In this study, we generated mutant strains of *S. praecaptivus* that lack the ability to produce or respond to a QS signaling molecule. We then used transcriptomics to determine the identities of genes in the bacterial genome that are regulated by QS. Wild type and mutant bacteria (defective in QS) were then microinjected into a model insect (the maize weevil, *Sitophilus zeamais*) which is known to have recently developed a symbiotic association with a close relative of *S. praecaptivus* (28). In contrast to a wild type strain, the QS mutant derivatives demonstrated a potent insect killing phenotype that is associated with the expression of several putative virulence determinants, including two encoding homologs of insecticidal proteins. The QS system was also demonstrated to induce suppression of bacterial growth *in vitro*, by enhancing expression of a gene (*cpmA*) with a cryptic amidohydrolase function. Suppression of virulence by the QS system in *S. praecaptivus* reduces the burden that these bacteria place on their insect host as their population density increases in host tissues, allowing them to maintain a benign and long-lasting infection.

3.3 Results

We show that *S. praecaptivus* and *S. glossinidius* maintain homologous quorum sensing systems. *S. glossinidius* has previously been shown, using mass spectrometric analysis, to produce N-(3-oxohexanoyl) homoserine lactone (OHHL) as a QS signaling molecule (13). The synthesis of OHHL is conducted by the protein product of the sogI gene [13], which shares 94% amino acid sequence identity with a gene designated *ypeI* (locus tag Sant_3558) in *S. praecaptivus*. Ethyl acetate extracts from both bacteria were separated on a thin layer chromatography (TLC) plate that was overlaid with a culture of an *Agrobacterium tumefaciens* reporter strain that degrades X-Gal in the presence of exogenous N-acyl HSL, yielding a blue color on the plate (Figure 3.1A). Since the extracts from *S. glossinidius* and *S. praecaptivus* each

produced a single co-migrating spot in this assay, we conclude that *S. praecaptivus* also produces only OHHL. We then confirmed that the enzyme encoded by the *ypeI* gene in *S. praecaptivus* is required for the synthesis of OHHL by generating a Δ*ypeI* knockout mutant strain using lambda Red recombineering. During growth in a liquid culture, the Δ*ypeI* strain failed to produce any signaling molecule that could be detected using the *A. tumefaciens* N-acyl HSL reporter strain (Figure 3.1B), confirming that the product of *ypeI* is responsible for synthesis of OHHL. *S. praecaptivus* also has two genes encoding candidate LuxR-like response regulators (*ypeR* and *yenR*; encoded by locus tags Sant_3587 and Sant_1175, respectively) that share high levels of amino acid sequence identity (93% and 92%, respectively) with previously characterized response regulators found in *S. glossinidius* (13). The amount of OHHL produced by *S. praecaptivus* was then measured over 11 hours of growth in liquid LB media, using the *A. tumefaciens* reporter strain. The amount of OHHL in the culture medium of the *S. praecaptivus* wild type (WT) strain increased in accordance with population density (Figure 3.1B). The Δ*ypeI* mutant strain growing under the same conditions did not produce any OHHL. However, curiously, it did display an increased growth rate relative to the WT strain. Together these results show that, like *S. glossinidius*, *S. praecaptivus* has an OHHL synthase encoded by its *ypeI* gene, along with a cognate response regulator (encoded by *ypeR*) and a disassociated second response regulator (encoded by *yenR*).

We conducted a transcriptomic analysis of the genes regulated by OHHL in *S. praecaptivus*. In order to identify genes whose expression is modulated by quorum sensing, we used a transcriptomic (RNA-Seq) approach to compare gene expression levels in a Δ*ypeI* mutant strain of *S. praecaptivus in vitro* in the presence or absence of 10 μg/ml OHHL, mimicking a high cell density state (with respect to QS). The 100 most significant results from this RNA-Seq experiment are presented in Table 3.1. A total of thirty genes were found to show significant differential expression with log2 fold changes >2 (Figure 3.2 (A)). The majority of these genes (26/30) demonstrated a decrease in expression in response to OHHL supplementation. Several of these genes are predicted to encode proteins that have functions associated with insecticidal activity and pathogenesis, the most notable of which are those predicted to encode homologs of

the PirA and PirB insecticidal toxins (Sant_2443, Sant_2444) that are known to play a role in insect killing in entomopathogenic *Photorhabdus* spp. (29). Other examples include genes encoding chitinases (Sant_1984, Sant_1963) and chitin binding domain-containing proteins (Sant_1090, Sant_P0292), which may play a role in degrading the insect integument (30) along with collagenase-like proteases (Sant_3444, Sant_3445), which may facilitate infiltration of host connective tissue (31). Several other genes whose transcripts were found to be downregulated in the presence of OHHL (i.e. under quorum) are anticipated to be involved in the formation of respiratory enzyme complexes. These genes encode components of the dimethyl sulfoxide reductase (Sant_0571, Sant_0570, Sant_0569, Sant_0568) and fumarate reductase (Sant_2415, Sant_2416, Sant_2417, Sant_2418) complexes. Other genes whose transcription was downregulated under quorum include a putative deoxyribonucleotide synthase (Sant_3837), two genes whose products are predicted to be involved in nitrogen metabolism (Sant_0171, Sant_2412), two genes whose products are predicted to play a role in regulating cell wall metabolism (Sant_2138, Sant_2857), a tRNA (*valY*), genes encoding a candidate metallophosphoesterase (Sant_P0288), a putative transcriptional regulator (Sant_3640), a putative colicin receptor (Sant_1851) and a putative citrate-succinate antiporter (Sant_2414).

Only four genes demonstrated a significant increase in expression in response to OHHL. Curiously, these include two genes (*cpmA* and *cpmJ*; Sant_3163, Sant_3164) that were shown to be induced by OHHL in *S. glossinidius* and are homologous to components of the carbapenem biosynthesis gene cluster that is present in a range of enteric bacteria (13). Based on the fact that both *S. praecaptivus* and *S. glossinidius* only maintain homologs of two genes from this biosynthetic pathway, we concur with the previously established hypothesis that these genes are not involved in antibiotic production and that they have some other unknown function that likely involves the predicted glutamine amidotransferase activity of CpmA (13). The other two genes demonstrating a significant increase in expression in response to OHHL include a putative carbon starvation protein (Sant_2155) and a putative autoinducer 2 kinase (Sant_3797) that may be involved in the regulation of another quorum sensing pathway.

In order to confirm the identities of genes regulated by QS, we performed a second

transcriptomic comparison using different *S. praecaptivus* mutant strains lacking each of the QS response regulators (YpeR and YenR). These mutant strains are expected to be impaired in their ability to facilitate the transcriptional changes that occur in the Δ*ypeI* mutant strain when OHHL is added to the culture. Furthermore, by comparing mutant strains that lack each response regulator, we can determine the contribution of each to the process of QS-mediated gene regulation. The data derived from comparative RNAseq analysis of the Δ*ypeR* and Δ*yenR* mutant strains are presented in Figure 3.2 (A) (for the top 30 most differentially expressed QS-regulated genes) and Table 3.2 (the 100 most significant results). Notably the genes that undergo significant changes in expression between the Δ*ypeR* and Δ*yenR* strains are a subset of the genes that undergo changes in expression in response to OHHL in the Δ*ypeI* mutant strain. While YpeR and YenR appear to influence the expression of the same genetic targets, the overall directionality of gene expression change indicates that the non-canonical response regulator (YenR) has a more potent impact. This is intriguing because it calls into question the purpose of maintaining two response regulators that modulate the expression of the same target genes. In addition, the amino acid sequences of YpeR and YenR share only 39 % sequence identity, suggesting that they did not arise as a consequence of a recent gene duplication event.

In order to validate the RNA-Seq transcriptomic data, we performed chitinase assays in WT *S. praecaptivus*, along with the Δ*ypeI*, Δ*ypeR* and Δ*yenR* mutant strains. As expected, the Δ*ypeI* strain had significantly more chitinase activity than a WT strain or a Δ*ypeI* strain grown in the presence of exogenous OHHL (Figure 3.2 (B)). This is consistent with the RNA-Seq data showing that the expression of chitinase genes is significantly reduced in a Δ*ypeI* mutant in the presence of OHHL. The Δ*ypeR* strain has a chitinase activity similar to the WT strain, indicating that YpeR has little influence on the regulation (repression) of chitinase activity under quorum. However, the Δ*yenR* strain and a Δ*yenR* Δ*ypeR* double mutant strain had significantly higher levels of chitinase activity under quorum, indicating that YenR is the main response regulator that represses chitinase production under quorum. This fits with the RNA-Seq data showing that the Δ*ypeR* mutant strain had lower numbers of chitinase gene transcripts (particularly for Sant_1984) relative to the Δ*yenR* mutant, consistent with the role of YenR in repression.

We show that the *S. praecaptivus* QS system controls a weevil killing phenotype. In order to determine how quorum sensing might impact the survival of *S. praecaptivus in vivo*, we microinjected equal numbers of WT and Δ*ypeI* strains into newly emerged adult grain weevils (*S. zeamais*) that were previously treated with rifampicin. Rifampicin treatment renders these weevils aposymbiotic by killing their native symbiont, *Candidatus* Sodalis pierantonius str. SOPE, which is a very close relative of *S. praecaptivus* (28) and is known to produce OHHL (13). The use of aposymbiotic weevils ensures that the results obtained in the current study only reflect the interaction between the weevil, *S. praecaptivus* and its endogenous QS system. In addition, symbiont-free weevils are considerably easier to inject because *Ca*. S. pierantonius str. SOPE provides the weevil with nutrients (aromatic amino acids) that harden the cuticle. Following microinjection, all weevils were maintained under identical conditions on a diet of organic maize in the absence of any antibiotic, and their mobility and survival was monitored daily (Table 3.4). Strikingly, at around one week following injection, weevils that were injected with the Δ*ypeI* mutant strain were observed to become lethargic (Figure 3.3). Over the course of the next seven days, all of the Δ*ypeI*-injected weevils succumbed to death (Figure 3.4 (A)). In contrast, weevils injected with the wild type strain suffered no lethargy or death over the course of experimental monitoring, aside from a small percentage of early deaths resulting from injuries sustained as a consequence of microinjection (<5%).

Injection of the Δ*ypeR* and Δ*yenR* mutant strains (lacking each of the *S. praecaptivus* QS response regulators) yielded a delayed/reduced weevil killing phenotype in comparison to the Δ*ypeI* strain, with the Δ*ypeR* strain demonstrating slightly more potent killing. However, a Δ*yenR* Δ*ypeR* double mutant was found to kill as effectively and rapidly as the Δ*ypeI* mutant (Figure 3.4 (A)). Further confirmation of the role of QS in weevil killing was obtained by injecting insects with a 1:1 mixture of WT and mutant bacteria (either Δ*ypeI*, Δ*ypeR* or Δ*yenR*). In these experiments, WT bacteria largely suppressed the killing effect of the Δ*ypeI* mutant, consistent with the notion that WT bacteria provide a source of exogenous OHHL that effectively complements the Δ*ypeI* mutant strain. However, the co-injection of WT bacteria along with the Δ*ypeR* or Δ*yenR* mutants did little to mitigate their killing phenoypes, consistent with the notion that the absence of a QS

response regulator cannot be complemented in this way (Figure 3.4 (B)). Taken together, the results of these microinjection experiments show that the genes involved in the *S. praecaptivus* QS system have a significant effect on weevil killing (see Tables 3.3 and 3.4 for data and statistical test results). They indicate that both YpeR and YenR respond to the OHHL synthesized by YpeI and act synergistically to reduce the expression of genes that are responsible for weevil killing, with YpeR having a more potent repressive effect.

We identified effector genes that are responsible for weevil killing. In order to identify the QS-regulated genes that are responsible for weevil killing (by the *ΔypeI* strain), we selected several candidate genes that displayed a significant change in expression in response to OHHL based on the transcriptomic data (Table 3.1) and might be expected to play a role in killing based on their anticipated functions. These candidate genes (from among those listed in Table 3.4) were then knocked out in a Δ*ypeI* mutant background and the resulting double mutants were inoculated into weevils to assess their killing capability. If a candidate gene plays a role in killing, then the resulting double mutant is expected to have a reduced killing capability relative to a *ΔypeI* single mutant strain. In this experiment, none of the double mutants that were tested *in vivo* were completely relieved of their weevil killing phenotype. However, the Δ*ypeI* Δ*regC*, Δ*ypeI* Δ*pirA* and Δ*ypeI* Δ*pirB* double mutant strains all demonstrated a statistically significant delay in killing relative to the Δ*ypeI* single mutant (Figure 3.4 (C); Tables 3.3 and 3.4). Furthermore, weevils injected with a Δ*ypeI* Δ*pirAB* mutant strain were found to have the same median longevity as weevils injected with either Δ*ypeI* Δ*pirA* or Δ*ypeI* Δ*pirB* double mutant strains, consistent with the notion that PirA and PirB constitute a binary toxin complex (requiring both toxin components for activity). Furthermore, a Δ*ypeI* Δ*pirAB* Δ*regC* triple mutant strain had a less potent killing phenotype than any of the double mutants, suggesting that RegC and PirAB function independently to effect killing. However, even this Δ*ypeI* Δ*pirAB* Δ*regC* triple mutant was not completely suppressed in weevil killing, suggesting that there are additional QS-regulated gene(s) that participate in killing that have not yet been identified in our study. Furthermore, although there is a general level of concordance between the transcriptomic data and the identification of genes involved in killing, it should be noted that our *in vitro* transcriptomic analysis revealed that

YenR has a more potent repressive effect on the transcription of *pirA*, *pirB* and *regC* under quorum (Table 3.2). However, the Δ*ypeR* strain has a more potent killing phenotype *in vivo*. This raises the possibility that the functions of the response regulators are different *in vivo*, at least with respect to their relative contributions to the process of QS-mediated gene regulation.

While it is beyond the scope of the current study to examine the role (in killing) of all genes that are differentially regulated by QS in *S. praecaptivus*, we did elect to test the effect of a Δ*ypeI* ΔSant_1962 double mutant, because Sant_1962 shares a high level of sequence identity with genes that are known to encode insecticidal delta endotoxins. In addition, its expression is reduced under quorum like that of *pirA* and *pirB*, albeit to a lesser extent (adjusted p = 0.09; Table 3.1). However, weevils injected with the Δ*ypeI* ΔSant_1962 double mutant had the same median lifespan as weevils injected with the Δ*ypeI* single mutant (Table 3.4), suggesting that Sant_1962 is not an effector of the QS-regulated mechanism of killing documented in this study. All other genes in the *S. praecaptivus* genome that are predicted (by virtue of homology) to function as toxins (Sant_0919, Sant_1053, Sant_2840) did not display significant reduction in expression in the presence of OHHL in the *in vitro* transcriptomic analysis (Table 3.1).

We show that quorum sensing suppresses the growth of *S. praecaptivus in vitro*. During the course of our experiments, we noticed that the rate of growth of the *S. praecaptivus* WT strain in liquid LB media was consistently lower than that of the Δ*ypeI* mutant (Figure 3.1 (B)). Furthermore, the addition of exogenous OHHL to LB plates was found to have a significant inhibitory effect upon the growth of both the *S. praecaptivus* WT and Δ*ypeR* mutant strains (Figure 3.5 (A)). However, the growth of the *S. praecaptivus* Δ*yenR* mutant was not suppressed by exogenous OHHL (Figure 3.5 (A)). In addition, the introduction of a plasmid overexpressing the OHHL synthase (YpeI) could only be achieved in a Δ*yenR* strain, presumably because the overexpression of this gene in a WT strain induces a severe growth defect, due to overproduction of OHHL. Furthermore, when this YpeI-overexpressing (Δ*yenR*) strain was streaked onto LB agar, it inhibited the growth of adjacent WT and Δ*ypeR* (but not Δ*yenR*) colonies (Figure 3.5 (B)). Since the Δ*yenR* mutant still produces OHHL due to the fact that it maintains an intact *ypeI* gene, the increased growth rate of the Δ*ypeI* mutant (relative to WT) cannot simply be explained as a

consequence of the loss of the metabolic burden associated with synthesizing OHHL. Rather, these results suggest that OHHL interacts with YenR, to modulate the transcription of target gene(s) that result in a suppression of growth.

Since none of the mutants that were screened in the weevil killing assays demonstrated an increased growth rate relative to the WT strain, we turned our attention towards genes that demonstrated a significant increase in transcript levels in the presence of OHHL. On LB agar plates supplemented with OHHL, we found that Δ*cpmA* and Δ*cpmAJ* mutant strains had an elevated growth rate relative to the WT strain (Figure 3.6). However, since a mutant lacking *cpmJ* alone demonstrated the same growth suppression as the WT strain in the presence of OHHL, it is clear that *cmpA* alone is responsible for the growth suppression phenotype. Furthermore, the Δ*cpmA* strain grew just as well as the Δ*yenR* strain in the presence of OHHL, in both solid (Figure 3.6) and liquid media (Figure 3.7), suggesting that *cpmA* is the only gene mediating the QS-associated growth suppression phenotype observed in our study.

We show that quorum sensing modulates bacterial population density *in vivo*, but not via CpmA. Given that the quorum sensing system in *S. praecaptivus* induces growth suppression *in vitro*, we sought to determine if it also affects the density of bacterial infection *in vivo*, following microinjection into weevils. This is an important question because an elevated density of bacterial infection would be anticipated to yield increased quantities of the PirAB toxin that is known to be involved in weevil killing. To investigate this issue, bacterial infection densities were estimated (only from live weevils) by plating the homogenates of surface sterilized insects on selective media and counting the colony-forming units obtained at intervals following microinjection. The resulting data (Figure 3.8 (A)) show that the WT strain maintains a consistent infection density in the weevil over the course of its lifespan, which equates to the lifespan of uninfected weevils (Table 3.4). However, the Δ*ypeR* strain displays a >10-fold increase in infection density (relative to WT) over the course of four weeks following injection and the Δ*yenR* strain achieves a ~2-fold increase (relative to WT) over the same time period. It should be noted that we could not obtain sufficient data for the Δ*ypeI* strain beyond two weeks following microinjection due to its potent killing phenotype. Contrary to what was observed in the *in vitro* experiments, the Δ*cpmAJ* strain

did not display an elevated growth *in vivo*, maintaining a similar infection density to the WT strain. In addition, the deletion of *cpmAJ* had no effect on weevil killing either when the mutation was introduced into a WT background or into a Δ*ypeI* background (Figure 3.4 (C)). Rather, the significant increases in infection densities observed with the Δ*ypeR* and Δ*yenR* strains are more readily explained as a consequence of the increased virulence properties of these mutants, highlighted by the fact that the increases in infection densities are most notable in the latter stages of infection, when the weevils are sick, presumably as a consequence of prolonged exposure to bacterial toxin(s) (Figure 3.8 (B)). These results, however, do not rule out the possibility that *cpmA* has a beneficial role in symbiosis. To this end, it is notable that the *cpmA* gene has been retained in an intact form in two insect symbionts that are closely related to *S. praecaptivus* (Figure 3.2 (A)).

3.4 Discussion

In the current study, we show that *S. praecaptivus* maintains an N-acyl HSL-based QS system that is genetically homologous to a system characterized previously in the derived insect symbionts, *S. glossinidius* and *Ca.* S. pierantonius str. SOPE (13). Microarray analysis of the *S. glossinidius* transcriptome revealed that the QS signaling molecule (OHHL) induced a substantial increase in the transcription of two genes of unknown function (*cpmA* and *cpmJ*) along with minor increases in the transcription of a wide range of genes involved in the cellular oxidative stress response (13). However, the inability to generate a mutant strain of *S. glossinidius*, lacking the OHHL synthase gene (*sogI*), compounded the analysis of the functions of this QS system *in vivo*. In the current study, we used an array of genetic and transcriptomic tools to investigate the homologous QS system in *S. praecaptivus*, yielding surprising insight into its functions *in vivo*.

Transcriptomic analysis of QS-defective mutant strains revealed that, at high bacterial population density, the *S. praecaptivus* QS system has a generally repressive effect upon the transcription of genes under its control. Furthermore, these analyses revealed that the QS system of *S. praecaptivus* does not significantly increase the transcription of genes involved in the bacterial oxidative stress response, indicating that this is a derived characteristic in *S. glossinidius*. We did however find that the QS system of *S. praecaptivus* drives an increase in

transcription of the enigmatic genes, *cpmA* and *cpmJ*, as previously observed in *S. glossinidius* (13), indicating that there is some functional synergy in the QS systems that are shared by these bacteria. Furthermore, in the current study, we found that *cpmA* mediates suppression of bacterial growth *in vitro* in response to the QS signal, OHHL. This suppression is eliminated in mutant strains lacking either *cpmA* or the gene encoding the QS response regulator (YenR) that increases *cmpA* transcription in response to OHHL. However, no enhancement of bacterial growth was observed following injection of a *cpmA* mutant strain into weevils. Curiously, in other Gram-negative bacteria, with the exception of members of the *Sodalis*-allied clade, homologs of *cmpA* and *cmpJ* constitute components of larger gene clusters encoding enzymes involved in the biosynthesis of the antibiotic, carbapenem (32,33). In this context, CpmA (also known as CarA in some bacteria) catalyzes the formation of a β-lactam ring using domains homologous to those of β-lactam synthase (B-LS) and asparagine synthetase (ASN) (34). The *S. praecaptivus* and *S. glossinidius* homologs of CpmA are highly conserved and both lack the region of the polypeptide encoding the B-LS domain, suggesting that they are not involved in β-lactam synthesis. Conservation of the ASN domain suggests that the function of CpmA involves amidohydrolase activity, which is known to be involved in a wide range of physiochemical processes in nature (35).

The transcriptomic analyses presented in this study show that the QS system of *S. praecaptivus* has some unique properties that have likely been lost in *S. glossinidius* as a consequence of the genome degeneration process that accompanies the transition to a static and obligate insect-associated lifestyle (14). Principal among these is the propensity for QS to downregulate the transcription of genes that are anticipated to have virulence properties, including insecticidal toxins and enzymes that are anticipated to degrade the insect integument. It was therefore of great interest to compare the effects of injecting WT and QS-deficient mutant strains of *S. praecaptivus* into an insect host. To achieve this goal, bacteria were injected into aposymbiotic maize weevils. This led to the striking finding that QS-deficient mutants have a potent weevil killing phenotype that is due, at least in part, to the action of genes encoding homologs of the binary insecticidal Pir toxins.

Genes encoding Pir toxins were initially identified in the entomopathogen *Photorhabdus luminescens* (29) and subsequently found in other bacteria including *Vibrio parahaemolyticus*, in which they play an important role in shrimp pathogenesis (36). It was shown that the crystal structure of the *V. parahaemolyticus* Pir toxins resembles that of the *Bacillus thuringiensis* Cry toxins, suggesting that they may have a conserved mode of action that ultimately causes destabilization of the host cell cytoskeleton, leading to cell death (37). Interestingly, *S. praecaptivus* also possesses a gene encoding a putative protein that shares substantial sequence identity with a Cry toxin. However, transcription of that gene is not controlled by QS and does not appear to play a role in the weevil killing phenotype described in this study. The only other gene identified to affect weevil killing in a QS-defective strain, annotated as *regC*, shares substantial sequence and structural homology with the bacteriophage P2 repressor that has a regulatory function. Thus, it seems unlikely that RegC is a direct effector of killing and more likely that it serves as a secondary regulator in the QS circuit, modulating the transcription of other genes that effect killing, perhaps including *pirA* and *pirB*. Indeed, a mutant strain lacking *ypeI*, *pirA*, *pirB* and *regC* displays a delayed killing phenotype relative to either a Δ*ypeI* Δ*pirAB* or a Δ*ypeI* Δ*regC* mutant strain, implying that RegC does influence the expression of effectors of killing other than just PirA and PirB. Clearly, further transcriptomic analyses are required to define the role of RegC in the process of killing. Moreover, based on the fact that the inactivation of *pirAB* and *regC* only delays the killing of weevils, rather than completely eliminating killing, it seems likely that there are additional virulence loci that remain to be identified that play a role in this process. Alternatively, it is possible that the weevil killing phenotype relies on a complex interplay of effectors that could not be investigated using our simple genetic screen.

It is pertinent to note that QS-mediated gene regulation is often used by bacterial pathogens to activate the expression of virulence factors at high bacterial population densities, in order to induce a concerted and potent attack on the host (4,38). However, our work shows that *S. praecaptivus* utilizes QS to reduce virulence gene expression when bacterial infection density increases in the host insect. This decoupling of virulence and infection density clearly facilitates *S. praecaptivus* maintaining a high density of infection in its host whilst minimizing negative

impacts on host fitness or longevity. Such a trait is anticipated to be particularly important for vector-borne parasites that need to maximize the fitness of their hosts as agents of dispersal (39). Indeed, it has been suggested that vector-borne parasites might even evolve positive impacts on host fitness to offset the metabolic cost of their passage (40). In such a scenario, a switch to vertical transmission would then be anticipated to effect the establishment of a mutualistic relationship. While the ecological underpinnings of the associations between *Sodalis*-allied symbionts and their insect hosts are not fully understood, it is clear that these bacteria have repeatedly and independently evolved mutualistic associations with insects that feed on a diverse array of plant and animal hosts (14). Based on the fact that *S. praecaptivus* was isolated from a human host and that its genome maintains a number of virulence genes that are normally found in plant pathogenic bacteria, we postulated that such mutualistic associations might have arisen from a context of vectorial transmission. Furthermore, close relatives of *S. praecaptivus* that have been found in certain stinkbugs and chestnut weevils have a low prevalence of infection within insect populations, consistent with the notion that these bacteria are not maternally inherited (in contrast to their mutualistic relatives) but are instead acquired from the environment by each new insect generation, presumably as a consequence of feeding on infected trees (24,27,41).

Based on the results of our study, it is also important to acknowledge that genes such as *pirAB* and *regC* must have a beneficial function in *S. praecaptivus* when they are expressed at low bacterial population densities. Given that low bacterial population density likely exists when insect hosts are initially infected, one explanation is that such virulence genes are required to assist bacteria in gaining entry into host tissues. Alternatively, these genes might play a role in host defense. In an elegant series of studies focusing on aphids, it was shown that a symbiotic bacterium named *Hamiltonella defensa* utilizes toxins to kill parasitoid wasps that attack its aphid host (42). The toxins utilized in this process are encoded by lysogenic bacteriophages (viruses) that are maintained by *H. defensa* and apparently induce relatively frequent bacterial cell lysis in order to synthesize (and liberate) their parasitoid-killing, toxic cargo (43). While we cannot rule out the possibility that *S. praecaptivus* or a derived, allied symbiont plays an analogous role in host defense, there are no such examples that have been reported to date involving these

bacteria. In addition, even the recently derived symbionts that are closely related to *S. praecaptivus* have lost many of the putative virulence genes (including *pirAB*) that are highlighted in our study, presumably as a consequence of the transition to permanent insect association, which removes the requirement for symbionts to participate in the initiation of infection.

3.5 Materials and Methods

Weevil rearing and maintenance were done as follows. *S. zeamais* weevils were reared on organic whole yellow maize (Purcell Mountain Farms) in an incubator at 27°C and 60% relative humidity. Symbiont-free (aposymbiotic) weevils were generated by rearing weevils on rifampicin treated corn that was prepared by hydrating dried corn with a 3% (w/v) solution of rifampicin (1mg/ml), prior to addition of insects. After three generations on this antibiotic diet, the loss of symbionts was confirmed by microscopic examination of 100 larvae (revealing absence of bacteriomes) and by negative PCR assays on whole weevil DNA using symbiont specific primers. Aposymbiotic insects were subsequently maintained on a normal diet and checked periodically to confirm the absence of symbionts.

Bacterial culture and genetic modification were done as follows. All strains of *S. praecaptivus* were cultured in LB media with appropriate antibiotics, unless otherwise described. Gene disruptions/deletions in *S. praecaptivus* were achieved using the lambda Red recombineering procedure, as described previously (44). Approximately 150 nucleotides of the 5' and the 3' of target genes were amplified by PCR with Phusion High Fidelity DNA Polymerase (Fisher Scientific). The 5' and 3' flanking sequences were then joined to an antibiotic resistance cassette (encoding either kanamycin, spectinomycin or gentamycin resistance) by PCR with Taq Polymerase MasterMix based on a previously described protocol [44]. The resulting construct was then electroporated into an *S. praecaptivus* strain harboring the lambda Red-Gamm plasmid, pRed/Gamm (CAT).

For transformation, *S. praecaptivus* cultures were grown in 25 ml 2YT5.8 media (20g/l Tryptone, 8g/l Yeast Extract, 10g/l NaCl, adjusted to pH 5.8) until their OD_{600} reached 0.4 units. Expression of lambda Red-Gamm proteins was then induced by addition of 0.4% arabinose for 30 minutes. Cells were harvested and washed twice in sterile ice cold water. DNA was

electroporated into cells using an Eppendorf electroporator model 2510, at 1600 V/s. Following a 1-hour recovery in SOC media, recombinant clones were then selected by plating on LB media with the appropriate antibiotic(s). Gene disruptions were verified by testing the linkage between the antibiotic resistance marker and the bacterial chromosome using PCR.

Cultures of the Agrobacterium tumefaciens KYC55 (pJZ372) (pJZ384) (pJZ410) reporter strain were grown in AT minimal media at 28°C (46), supplemented with 1.5µg/ml of tetracycline, 100 µg/ml of gentamycin and 100 µg/ml of spectinomycin (13).

OHHL extraction and TLC assay were performed as follows. OHHL extraction was performed on culture supernatants based on a previously described procedure [45]. Briefly, 25 ml cultures of *S. glossinidius* (grown in liquid MM medium, at 25°C and 200 rpm shaking) and *S. praecaptivus* (grown in LB medium, at 30°C and 200 rpm shaking) were pelleted by centrifugation (8,000g, 20 min., 4°C) once their turbidity reached an $O.D_{600}$ of 0.4 units. The resulting culture supernatants were filtered through 0.22 micron pore-size membrane filters (Argos Technologies) and then extracted by shaking with an equal volume of ethyl acetate for 30 minutes. The ethyl acetate extracts were dried with anhydrous magnesium sulfate and filtered. The solvent was then evaporated using a vacuum centrifuge at 60°C and the OHHL-containing residue was resuspended in 100 µl of methanol. These extracts were then subjected to thin layer chromatography on a C_{18} reverse-phase TLC plate (Whatman) using methanol:water (60:40) as the solvent/carrier. Following development, the plate was dried and overlaid with a live culture of an *A. tumefaciens* acyl-HSL reporter strain as described previously [46].

OHHL bioassays were done as follows. The wild type and Δ*ypeI* strains of *S. praecaptivus* were cultured overnight in 10 ml LB liquid media from single colony inoculations. These cultures were washed, resuspended and used to start 50 ml cultures, at OD_{600} of 0.03 units. During an 11-hour incubation with shaking at 200 rpm and 30°C, the cultures were sampled every 2 hours to check cell density and assay for the presence of OHHL with the β-galactosidase activity (Miller) assay (48) using an *A. tumefaciens* acyl-HSL reporter strain, KYC55 (pJZ372)(pJZ384)(pJZ410), as described previously [46]. The extraction of OHHL was performed from 900 µl of supernatant from the *S. praecaptivus* cultures into 100 µl of methanol. Following

this, 5ml cultures of the *A. tumefaciens* acyl-HSL reporter strain (starting OD_{600} of 0.03) were exposed to 10 µl of the OHHL extracts for 12 hours at 200 rpm shaking, prior to performing β-galactosidase assays. OHHL concentration was also measured for *S. praecaptivus* wild type cultures of 20 ml, grown for four hours at 200 rpm shaking and 30°C to OD_{600} of 0.4. The extraction of OHHL was performed from total culture supernatant into 200 µl of methanol, which was then used as substrate in the *A. tumefaciens* /β-galactosidase assay. Solutions of 50, 500 and 1250 nM OHHL (Sigma Aldrich, K3255) were prepared in methanol for use as standards. The concentration of OHHL in the OD_{600} = 0.4 culture was determined to be ~1 µg OHHL/ml.

Transcriptomics assays were performed as follows. 20 ml cultures of *S. praecaptivus* were grown in LB media, at 200 rpm shaking and 30°C, with or without supplementation with OHHL (10 µg /ml), which represents ten times the concentration found in the *S. praecaptivus* culture at an $O.D_{600}$ = 0.4, based on the bioassay described above. Total nucleic acid extraction was performed on each culture as described previously, after four hours of growth for the experiment involving the Δ*ypeI* strain or five hours of growth for the experiments involving the Δ*ypeR* and Δ*yenR* strains (49). RNA was extracted using the Purelink RNA minikit (Ambion) according to the manufacturer's instructions. The resulting RNA was analyzed using an Agilent bioanalyzer to ensure that it lacked DNA contamination and was of sufficient quality for cDNA preparation. Total RNA samples were then submitted to the core sequencing facility at University of Utah for Illumina TruSeq library preparation and sequencing on a HiSeq instrument (Illumina). The resulting 50-base single reads were filtered using NGSQCToolkit (50) and mapped to the reference genome sequence using bowtie2 (51) employing the --very-sensitive preset. Read counts mapping to individual genes were generating using HTSeq (52) by running htseq-count using the options -s no -a 0 -m intersection-nonempty -t gene. Next, using custom Perl scripts, counts from three biological replicate cultures were combined and subject to statistical analysis. After normalization, combined counts files were compared using DESeq2 (53).

Chitinase assays were done as follows. Chitinase activities in the *S. praecaptivus* culture supernatants were measured using a fluorimetric assay (Sigma-Aldrich, CS1030) according to the manufacturer's instructions. Cells were grown in LB media (15 ml volume), from a starting OD

$_{600}$ of 0.05, with 200 rpm shaking at 30°C until O.D $_{600}$ reached ~1 unit. Then, 10 µl of culture supernatant was added to 90 µl of the substrate working solution (containing 4-methylumbelliferyl β-D-N, N-diacetylchitobioside hydrate) in a 96-well fluorescence plate (Greiner Bio-One, 655096) and incubated for 60 minutes at 37 °C in the dark. The reaction was stopped by adding 200 µl of sodium carbonate buffer, and the fluorescence was measured with a SynergyMx plate reader (BioTek Instruments Inc.) within 15 minutes of the reaction end point. The chitinase activity was calculated using the 100 ng 4-methyl umbelliferone standard.

Growth suppression assays were performed as follows. Plate growth assays were performed by spotting appropriate dilutions of overnight cultures, on plates containing LB agar without sodium chloride (to inhibit swarming motility). OHHL supplementation was achieved by pipetting OHHL directly onto plates or impregnating sterile paper strips on the surface of the plates after soaking them in 10 mg/ml OHHL in methanol. Controls were performed using an equivalent volume of methanol alone. Recombinant *S. praecaptivus* strains were also used as a source of OHHL by streaking bacteria onto plates for testing. One of these recombinant strains maintains a pCM66 plasmid expressing *ypeI* in a Δ*yenR* background and can therefore overproduce OHHL without undergoing YenR-mediated growth suppression. The other strain maintains an empty pCM66 plasmid in a Δ*ypeI* background and therefore does not produce any OHHL. All plates in these experiments were incubated at 30°C.

Liquid culture assays were done by growing the appropriate bacterial strains until their OD_{600} reached 0.3 and then splitting them in two equal volumes of 20 ml and supplementing the resulting cultures either with 200 µl of 10 mg/ml OHHL (100 µg/ml final concentration in media) or an equal volume of water. The turbidity of each culture was then monitored over a five hour period during incubation with shaking at 200 rpm at 30°C.

Weevil microinjections were performed as follows. Newly emerged adult aposymbiotic weevils were used for all microinjection experiments because these insects have a significantly thinner cuticle relative to their symbiotic counterparts, facilitating a substantially higher level of survival following microinjection. Capillary tubes (3.5” Drummond # 3-000-203-G/X, Drummond Scientific Company) were pulled to create a short sharp tip (Bee-Stinger needle) with Micropipette

puller P-97 (Sutter Instruments). The settings on the micropipette puller were as follows: Heat=292, Pull=100, Velocity=60, Time=250, Pressure=500. Weevils were immobilized by a brief incubation on ice and the needle was immersed in 50µl of an overnight bacterial culture to collect bacteria by capillary action. The needle was then used to pierce the cuticle of the weevils in the thoracic region between the middle and hind legs. This resulted in a median 2800 bacterial cells being transferred into each weevil, as observed by plating weevil homogenates directly after injection. Following injection, weevils were then transferred to hydrated maize grains and maintained in an incubator at 27°C and 60% relative humidity. The cultures were inspected weekly to assess weevil mortality following injection.

Bacterial isolation from weevils was done as follows. Surface contaminants were removed from weevils by immersing the adult insects in a solution of 10% bleach for 5 minutes with agitation using a magnetic stir bar. Weevils were then air dried and homogenized in 100µl of sterile water. A dilution series was plated on LB agar (without sodium chloride) containing 50µg/ml polymyxin B to select for *S. praecaptivus*.

Weevil morbidity assessment was performed as follows. Individual weevils were placed in the center of an empty petri dish and the time taken for them to move from the center of the dish to the periphery was recorded. Any weevils that displayed no sign of movement during the assay were excluded from the experiment.

3.6 Acknowledgements

We thank Kelly Hughes for the provision of plasmids used in this study.

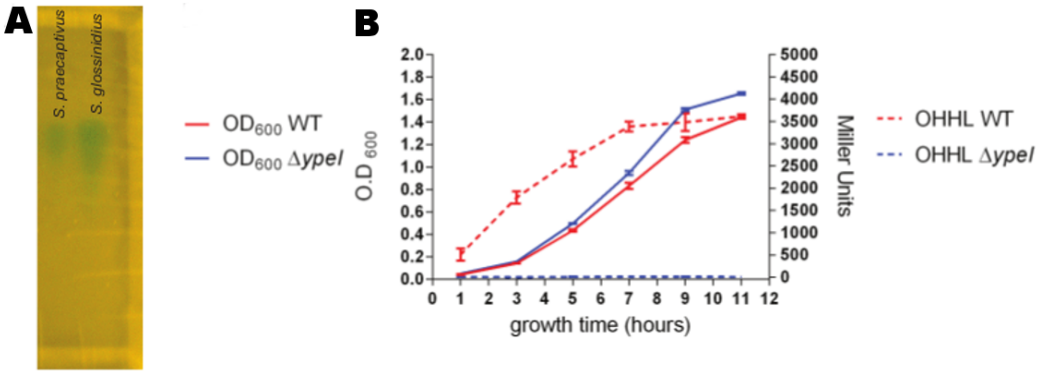

Figure 3.1. Characterization of the *S. praecaptivus* QS system. (A) TLC plate with ethyl acetate extracts derived from culture supernatants of *S. praecaptivus* and *S. glossinidius*. The plate was overlaid with an *A. tumefaciens* AHL reporter strain that produces blue spots in the presence of AHL molecules. This assay shows that *S. praecaptivus* and *S. glossinidius* each produce a single AHL molecule, which was previously characterized as OHHL in *S. glossinidius* (13). (B) Growth (OD_{600}) and OHHL production (assayed using the *A. tumefaciens* reporter strain) of WT *S. praecaptivus* and an isogenic strain lacking the putative OHHL synthase (Δ*ypeI*). Data were obtained from three biological replicates and error bars show standard deviations.

Table 3.1. OHHL dependent transcriptomes of ΔypeI mutant strain.

Locus	Gene name	Predicted product	ct NOOHHL 3	ct NOOHHL 2	ct NOOHHL 1	ct OHHL 3	ct OHHL 2	ct OHHL 1	padj	log2 Fold change
Sant_P0292	-	Fibronectin type III domain-cntnng. protein	3161.674	2386.97	3353.98	112.2	155.3	53.91	1.70E-32	4.06066
Sant_1984	-	Putative exochitinase	3105.555	2541.09	3359.693	177.9	241.06	143.7	5.36E-33	3.56756
Sant_0571	dmsA1	Put. Dimeth. sulfox. Reduct. major subunit	1472.107	758.379	2027.63	66.5	97.46	105	2.19E-21	3.36117
Sant_2415	frdA	Fumarate reductase subunit A	1558.289	591.103	1999.05	58.19	129.9	68.09	2.40E-16	3.21556
Sant_2444	pirA	JHE-like toxin	171.3617	142.8421	192.4725	7.4814	20.142	5.674	6.73E-17	3.16055
Sant_2414	-	Putative anion transporter	1452.065	833.559	2616.483	66.5	153.99	126.7	9.67E-16	3.09688
Sant_2443	pirB	JHE-like toxin	681.4384	583.5851	689.852	42.394	87.066	43.5	8.87E-20	3.02496
Sant_2416	frdB	Fumarate reductase subunit B	530.119	171.035	554.55	20.78	51.98	11.35	1.23E-11	2.92189

Note: Cultured in the presence or absence of OHHL, ranked according to log2fold change in transcript numbers (first hundred results). Three biological replicates were performed for each condition and the columns containing count data are labeled ctOHHL1-3 (for cultures with OHHL) or ctNOOHHL1-3 (for cultures lacking OHHL).

Table 3.1. (Continued)

Locus	Gene name	Predicted product	ct NOOHHL 3	ct NOOHHL 2	ct NOOHHL 1	ct OHHL 3	ct OHHL 2	ct OHHL 1	padj	log2 Fold change
Sant_2418	frdD	Fumarate reductase subunit D	209.4421	62.96329	222.96321	9.1439	18.843	10.403	1.19E-11	2.83325959
Sant_1851	ompW	Outer membrane protein	3157.665	2090.005	4975.7003	231.09	435.98	347.08	1.14E-15	2.83060008
Sant_2417	frdC	Fumarate reductase subunit C	219.4633	79.8788	272.51059	8.3126	29.239	4.7286	1.81E-09	2.70796815
Sant_3640	regC	Prophage P2 protein	148.3131	98.67381	163.88749	17.456	17.543	9.4571	1.03E-13	2.68123125
Sant_1090	-	Putative chitin-binding domain 3 protein	102.2158	74.2403	85.755079	9.9751	13.645	5.6743	6.54E-12	2.58890469
Sant_0569	dmsC	DMSO reductase anchor subunit	221.4675	84.57755	219.15187	17.456	25.99	19.86	1.29E-10	2.49229026
Sant_1963	-	Chitinase	99.20942	54.50553	108.6231	14.131	11.695	8.5114	6.19E-10	2.39133524
Sant_0568	dmsD	Twin-argninine leader-binding protein	166.3511	58.26454	165.79315	13.3	19.492	17.969	4.12E-09	2.3640079

Table 3.1. (Continued)

Locus	Gene name	Predicted product	ct NOOHHL 3	ct NOOHHL 2	ct NOOHHL 1	ct OHHL 3	ct OHHL 2	ct OHHL 1	padj	log2 Fold change
Sant_2412	nasB	Nitrite reductase	325.68749	219.9016	617.43657	49.876	55.878	64.31	4.86E-10	2.322843
Sant_P0288	-	Metallophosphoesterase	317.67056	217.0824	352.54866	42.394	64.975	32.15	6.50E-11	2.2867733
Sant_3445	-	Peptidase U32	204.43153	107.1316	230.58588	21.613	29.239	32.15	4.27E-10	2.2861539
Sant_2138	lytS	Signal transduction histidine kinase	117.24749	76.1198	123.86845	19.119	15.594	16.08	4.60E-10	2.2445433
Sant_0570	dmsB	Anaer. Dimeth. Sulfox. reductase chain B	325.68749	138.1433	343.02032	35.744	62.376	26.48	3.71E-08	2.1938857
Sant_3444	yhbU	Peptidase U32	199.42095	140.9626	259.17091	27.432	30.538	48.23	2.23E-09	2.1386482
Sant_3837	-	Anaer. ribonuc.-triphosph. reductase	282.59653	179.4924	491.66246	35.744	70.173	59.58	9.85E-08	2.0846682
Sant_0171	-	Nitrate reductase 2 alpha subunit	937.97996	510.2846	1248.2128	147.96	217.67	127.7	1.61E-08	2.0804602

Table 3.1. (Continued)

Locus	Gene name	Predicted product	ct NOOHHL 3	ct NOOHHL 2	ct NOOHHL 1	ct OHHL 3	ct OHHL 2	ct OHHL 1	padj	log2 Fold change
valY	valY	-	185.3913	268.76867	409.7187	59.85	34.437	64.308	3.02E-08	2.068508
Sant_1414	fruB	PTS fam. fruct. porter; IIA/HPr component	65.1375	59.204287	202.0009	16.63	14.944	19.86	NA	2.067981
Sant_2857	-	Putative phage lysozyme	56.11846	40.409275	66.6984	9.975	11.695	6.62	4.30E-07	2.031905
Sant_ps0811	-	-	32.06769	20.674513	47.64171	4.156	4.5482	7.5657	NA	1.975177
Sant_0172	-	Cryptic nitrate reductase 2 subunit beta	331.7002	182.31161	392.5677	58.19	77.32	46.34	6.60E-08	1.973141
Sant_2464	ycfP	Hypothetical protein	153.3236	137.20359	299.1899	29.09	42.234	46.34	2.38E-07	1.953524
Sant_2000	ynfK	Putative dethiobiotin synthase	191.404	265.94942	365.8883	52.37	52.63	75.657	6.47E-08	1.898075
Sant_3652	uxaC	Glucuronate isomerase	595.2565	577.94661	1131.967	100.6	259.25	102.14	NA	1.893857

Table 3.1. (Continued)

Locus	Gene name	Predicted product	ct NOOHHL 3	ct NOOHHL 2	ct NOOHHL 1	ct OHHL 3	ct OHHL 2	ct OHHL 1	padj	log2 Fold change
Sant_0173	-	Nirate reductase delta subunit	123.2602	64.84279	150.5478	21.613	31.188	16.077	2.22E-06	1.88066
valU	valU	-	129.2729	172.9141	301.0956	54.863	24.041	47.286	3.04E-06	1.865321
Sant_2137	-	AraC family transcriptional regulator	142.3004	53.56578	125.7741	22.444	22.091	22.697	3.07E-06	1.861865
Sant_3838	-	Anaer. ribonuc.-triphosph. red. Act. protein	49.10365	46.04778	72.4154	11.638	11.046	12.294	2.22E-06	1.861793
valX	valX	-	237.5013	356.1655	466.8888	84.789	64.975	91.734	8.16E-08	1.860095
Sant_2623	-	hypothetical protein	95.20096	90.21606	156.2648	24.107	32.487	17.023	1.07E-06	1.848795
csrB	csrB	-	3816.055	5434.578	7891.373	1141.3	1402.8	1517.9	7.51E-08	1.825254
Sant_2803	-	Putative chitinase	128.2708	96.79431	114.3401	17.456	37.036	23.643	1.20E-06	1.79851

Table 3.1. (Continued)

Locus	Gene name	Predicted product	ct NOOHHL 3	ct NOOHHL 2	ct NOOHHL 1	ct OHHL 3	ct OHHL 2	ct OHHL 1	padj	log2 Fold change
Sant_3651	uxaB	Altronate oxidoreductase	319.6748	314.8164	512.62481	63.1759	133.85	66.2	1.89E-06	1.796928
Sant_3653	exuT	D-galactonate transporter	348.7361	327.973	426.86973	70.6573	128.65	70.928	3.48E-07	1.768271
Sant_2456	pepT	Peptidase T	250.5288	268.7687	442.11508	69.826	59.777	104.03	1.03E-06	1.7629
Sant_3971	-	1;4-dihyd.-2-naphth. octaprenyltransferase	194.4104	205.8054	384.94502	59.0196	59.777	71.874	1.03E-06	1.759215
Sant_3366	leuA	2-isopropylmalate synthase	156.33	142.8421	259.17091	41.5631	46.782	52.014	1.15E-06	1.723207
ssrS	ssrS	-	1554.281	2022.343	3904.7146	527.851	831.68	449.21	1.17E-05	1.721179
Sant_2767	cydA1	Cytochrome d ubiquinol oxidase subunit I	1936.087	1612.612	2498.3313	541.983	398.95	679.97	4.30E-07	1.683185
Sant_0455	-	hypothetical protein	49.10365	27.25277	53.358716	9.14388	14.944	6.62	NA	1.618989

Table 3.1. (Continued)

Locus	Gene name	Predicted product	ct NOOHHL 3	ct NOOHHL 2	ct NOOHHL 1	ct OHHL 3	ct OHHL 2	ct OHHL 1	padj	log2 Fold change
Sant_0800	-	hypothetical protein	281.5944	286.62393	623.15358	78.97	150.7	95.517	NA	1.562429
Sant_1834	adhE	Bifunct. acetald.-CoA/alc. dehydrogenase	695.468	608.01863	2111.4806	233.58	366.5	293.17	0.000508	1.557598
Sant_2688	dps	DNA starv./station. phase protect. protein	1072.263	805.36626	1827.536	169.58	544.5	262.91	0.0004569	1.556644
Sant_2637	pflB	Formate acetyltransferase 1	2818.95	1615.4313	4413.5281	748.97	501.6	1169.8	0.0002668	1.547153
Sant_3781	fucO	L-1;2-prop. oxidoreduct.; lactald. reductase	207.4379	140.96259	371.60534	52.369	92.91	51.068	0.0002452	1.543881
Sant_2766	cydB1	Cytochrome d ubiquinol oxidase subunit II	1091.304	863.63079	1358.7416	367.42	229.4	389.63	7.43E-06	1.542728
Sant_1336	yfbU	YfbU family protein	165.349	157.8781	304.90695	49.876	61.08	69.983	4.00E-05	1.540774
Sant_1415	fruK	1-phosphofructokinase	41.08673	16.915511	142.92513	20.782	12.99	11.349	0.0064197	1.49739

Table 3.1. (Continued)

Locus	Gene name	Predicted product	ct NOOHHL 3	ct NOOHHL 2	ct NOOHHL 1	ct OHHL 3	ct OHHL 2	ct OHHL 1	padj	log2 Fold change
Sant_0277	ilvG	Acetolactate synth. isozyme II large subunit	112.2369	101.4931	146.7365	36.576	37.685	36.883	2.39E-05	1.4842
Sant_2765	ybgT	cyd operon protein YbgT	99.20942	82.69805	123.8684	39.069	18.193	34.991	0.00024053	1.47094
Sant_2184	-	TIM-barrel signal transduction protein	145.3067	187.0104	306.8126	37.407	107.86	33.1	0.00199501	1.45574
Sant_2569	-	hypothetical protein	39.0825	37.59002	78.13241	14.131	5.8477	22.697	0.00308128	1.44909
Sant_0174	narV	Nitrate reductase gamma subunit	117.2475	46.98753	137.2081	19.95	38.335	28.371	0.00139881	1.4456
Sant_1357	menH	2-s.-5-e.-6-h.-3-c.-1-carboxylate synthase	113.239	117.4688	188.6612	35.744	40.284	55.797	0.00016187	1.43738
Sant_0025	agaS1	Tag.-6-phosph. ket./ald. isomerase	161.3406	129.6856	242.0199	45.719	85.767	27.426	0.00139578	1.42099
Sant_2636	focA	Formate transporter	316.6684	260.3109	398.2847	97.258	63.675	150.37	0.00030847	1.41556

Table 3.1. (Continued)

Locus	Gene name	Predicted product	ct NOOHHL 3	ct NOOHHL 2	ct NOOHHL 1	ct OHHL 3	ct OHHL 2	ct OHHL 1	padj	log2 Fold change
Sant_1337	-	Putative phosphatase	143.30249	128.7458	243.92556	58.188	53.929	57.688	0.00024053	1.38511
Sant_0424	bfrA	Bacterioferritin	393.83133	416.3095	808.00341	116.38	266.4	127.67	0.00161072	1.378018
Sant_0812	-	Put. phage-rel. transmem. protein	23.048653	14.09626	19.056684	5.8188	7.1472	1.8914	NA	1.372173
Sant_1922	pntA	NAD(P) transhydrogenase subunit alpha	681.43843	604.2596	1027.1553	230.26	284.59	282.77	7.35E-05	1.364823
Sant_0276	ilvX	expressed protein ilvX	5.0105767	6.578254	5.7170053	0	0.6497	1.8914	NA	1.357202
Sant_3972	rraA	Ribonuclease activity regulator protein	353.74671	404.0928	596.47422	152.12	155.94	162.66	7.35E-05	1.356026
Sant_2183	-	hypothetical protein	145.30672	187.0104	312.52962	39.901	118.25	39.72	0.00495398	1.351306
Sant_0024	agaV	NAG-spec. enz. IIB cmpnt of PTS	79.167112	90.21606	142.92513	19.95	59.777	14.186	0.00773629	1.336626

Table 3.1. (Continued)

Locus	Gene name	Predicted product	ct NOOHHL 3	ct NOOHHL 2	ct NOOHHL 1	ct OHHL 3	ct OHHL 2	ct OHHL 1	padj	log2 Fold change
Sant_1298	yfcZ	TRNA-dihydrouridine synthase A	122.25807	120.2881	194.37818	43.226	61.726	44.448	0.000470	1.3319566
Sant_3442	yhbS	Putative acetyltransferase	86.181919	55.44528	133.39679	38.238	27.289	26.48	0.002476	1.3079416
Sant_0106	-	Aldehyde dehydrogenase family protein	663.40035	655.0062	1486.4214	170.41	560.08	118.21	0.014076	1.3078212
Sant_3174	raiA	Putative sigma-54 modulation protein	1917.0466	2039.259	4524.0569	722.37	1404.1	743.33	NA	1.2997654
Sant_2442	-	hypothetical protein	17.035961	13.15651	13.339679	4.9876	3.8985	3.7828	NA	1.2913438
Sant_3594	dkgA	2;5-diketo-D-gluconate reductase A	648.36862	697.2949	1046.212	168.75	456.12	199.55	0.003826	1.2806439
Sant_1580	-	Endo/exonucl./phosphat. fam. protein	101.21365	105.2521	270.60492	43.226	73.421	43.503	NA	1.2688344
Sant_3443	yhbT	Putative sterol transferase	164.34692	160.6974	301.09561	64.007	90.965	69.983	0.001421	1.2660344

Table 3.1. (Continued)

Locus	Gene name	Predicted product	ct NOOHHL 3	ct NOOHHL 2	ct NOOHHL 1	ct OHHL 3	ct OHHL 2	ct OHHL 1	padj	log2 Fold change
Sant_2049	pykF	Pyruvate kinase	707.4934	639.9702	996.6646	262.679	270.295	345.185	0.000241	1.265886
Sant_0199	uspA	Universal stress protein A	797.6838	925.6543	2073.367	267.666	736.1641	269.528	0.012748	1.250314
Sant_1359	menB	Naphthoate synthase	157.3321	121.2278	165.7932	57.3571	50.03057	60.5255	0.000471	1.245765
Sant_r0474	-	-	722.5252	873.968	1269.175	361.599	336.5693	390.579	0.000385	1.244345
Sant_r0265	-	-	661.3961	888.0643	1255.835	332.505	324.8738	402.873	0.000639	1.241379
Sant_3780	-	MaoC domain protein dehydratase	48.10154	31.95152	47.64171	6.65009	23.39092	12.2942	NA	1.240837
Sant_2233	-	Put.3-oxoacid CoA-transf.;β subunit	49.10365	62.02354	78.13241	14.1315	36.38587	14.1857	0.009807	1.232437
Sant_4024	-	hypothetical protein	302.6388	320.455	514.5305	87.2825	233.2594	83.2226	0.009732	1.220188

Table 3.1. (Continued)

Locus	Gene name	Predicted product	ct NOOHHL 3	ct NOOHHL 2	ct NOOHHL 1	ct OHHL 3	ct OHHL 2	ct OHHL 1	padj	log2 Fold change
Sant_3269	garL	2-dehyd.-3-deoxygluc. aldolase	56.11846	56.385	104.8118	16.6252	38.3351	20.8056	0.0096058	1.2181457
Sant_3982	pfkA	6-phosphofructo kinase	748.5802	842.956	1863.744	379.055	451.575	452.05	0.0040782	1.217225
Sant_P0204	-	hypothetical protein	104.22	51.6863	66.6984	26.6004	33.7869	21.7514	0.006119	1.2082931
Sant_2570	-	Stress induced protein	57.12057	110.891	184.8498	19.119	74.721	19.8599	0.0331567	1.2068822
Sant_0023	agaW	PTS sys. NAG-spec. IIC component	166.3511	139.083	213.4349	50.707	106.559	28.3713	0.0130996	1.1972223
Sant_r3942	-	-	515.0873	590.163	901.3812	265.173	237.158	292.225	0.0011303	1.1859228
Sant_r0476	-	-	692.4617	831.679	1280.609	361.599	315.128	431.244	0.0016107	1.181864
Sant_2166	-	Urocanate hydratase	186.3935	212.384	278.2276	73.151	118.254	73.7655	0.0023335	1.1768695

Table 3.1. (Continued)

Locus	Gene name	Predicted product	ct NOOHHL 3	ct NOOHHL 2	ct NOOHHL 1	ct OHHL 3	ct OHHL 2	ct OHHL 1	padj	log2 Fold change
Sant_r0930	-	-	700.4786	850.4743	1200.571	344.1424	309.9296	442.593	0.0013958	1.1765077
Sant_2232	-	Putative coenzyme A transferase	51.10788	79.8788	89.56642	25.76912	35.73612	21.7514	0.0067061	1.1747892
Sant_3367	leuB	3-isopropylmalate dehydrogenase	60.12692	44.16828	121.9628	29.92543	28.5889	24.5885	0.0135024	1.1652174

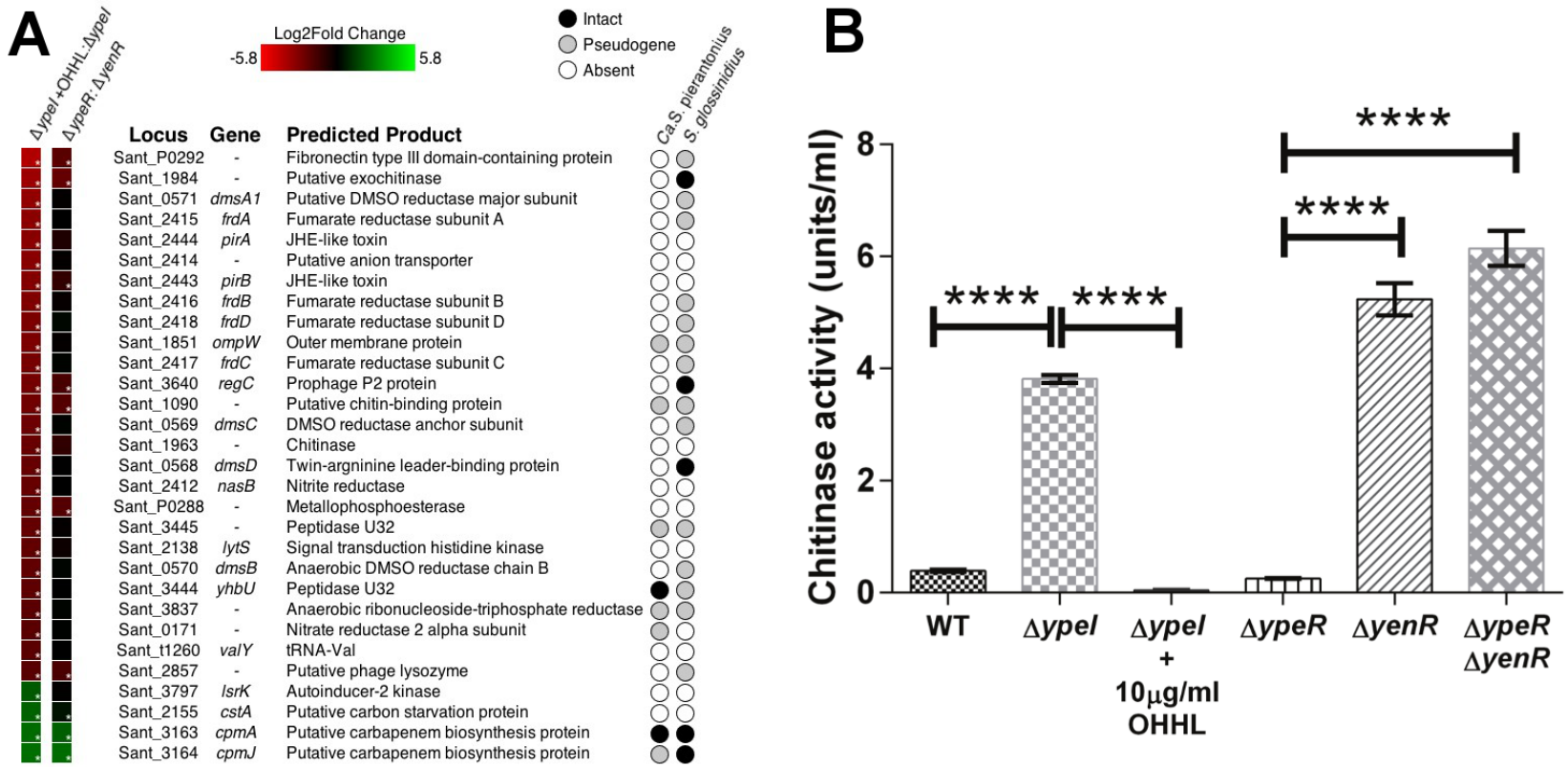

Figure 3.2. Transcriptomic (RNA-Seq) analysis of genes mediating QS in *S. praecaptivus*.
(A) Heat map showing changes in expression of the top 30 (most differentially expressed) genes in *S. praecaptivus* in response to OHHL. The asterisks in the boxes on the left indicate statistically significant levels of differential expression. The matrix on the right-hand side of the panel shows the status of genes in *Sodalis*-allied insect symbionts that are closely related to *S. praecaptivus*. (B) Chitinase activities of WT and mutant *S. praecaptivus* strains, in the presence or absence of OHHL. All samples were assayed in triplicate and error bars show standard deviations. Ordinary one way ANOVA comparisons between genotypes: Δ*ypeI* vs. Δ*ypeI* supplemented with 10 μg/ml OHHL, WT vs. Δ*ypeI*, Δ*ypeR* vs. Δ*yenR* and Δ*ypeR* vs. Δ*ypeRyenR*, all yield P <0.0001; Δ*yenR* vs. Δ*ypeR* Δ*yenR* double mutant yields P = 0.0006.

Table 3.2. Transcriptomic comparison of ΔyenR and ΔypeR mutant strains.

Locus	Gene name	product	ctYpeR 3	ctYpeR 2	ctYpeR 1	ctYenR 3	ctYenR 2	ctYenR 1	padj	log2 Fold change
Sant_1984	-	Putative exochitinase	324.45	247.79	208.47	2416.58	2807.5	1902.77	3.14E-36	-2.28258
Sant_P0292	-	Fibronectin t. III dmn.-cng. protein	251.73	155.66	138.67	1803.43	2189.03	1569.46	1.81E-26	-2.09142
Sant_1090	-	Put. chitin-binding domain 3 protein	27.038	26.474	30.711	173.042	207.058	126.305	8.71E-30	-1.95585
Sant_P0288	-	Metallo phosphoesterase	158.5	146.13	112.61	593.143	702.552	550.831	1.42E-60	-1.94044
Sant_2857	-	Putative phage lysozyme	14.917	13.766	18.613	85.0205	113.023	78.356	8.45E-19	-1.70044
Sant_3640	regC	Prophage P2 protein	50.346	47.652	37.226	196.047	197.112	162.56	6.27E-27	-1.67433
Sant_1258	-	Peptidase M60 vir. enh. protein	116.54	111.19	84.689	400.096	357.153	295.882	6.60E-31	-1.54172
Sant_2856	-	D-isomer specific 2-hydroxyacid dehydrogenase NAD-binding protein	35.429	36.004	28.85	115.028	156.424	100.576	1.57E-15	-1.42944

Note: Ranked according to log2fold change in transcript numbers (first hundred results). Three biological replicates were performed for each strain and the columns containing count data are labeled ctYenR1-3 (for Δ*yenR* strain) and ctYpeR1-3 (for Δ*ypeR*)

Table 3.2. (Continued)

Locus	Gene name	product	ctYpeR 3	ctYpeR 2	ctYpeR 1	ctYenR 3	ctYenR 2	ctYenR 1	padj	log2 Fold change
Sant_0455	-	hypothetical protein	9.3233	18.002	13.96	79.019	54.251	54.966	NA	-1.33635
Sant_2803	-	Putative chitinase	55.94	49.77	30.711	230.06	197.11	147.36	6.58E-10	-1.28903
Sant_ps0811	-	-	25.173	14.825	12.098	62.015	85.898	53.797	NA	-1.22704
Sant_2443	pirB	JHE-like toxin	49.414	29.65	32.573	135.03	92.227	105.25	3.63E-10	-1.16951
Sant_1963	-	Chitinase	15.85	24.356	23.266	67.016	88.61	47.949	NA	-1.09818
Sant_0813	-	Protein gp55	22.376	16.943	14.89	58.014	57.868	44.441	NA	-0.9911
Sant_0273	-	hypothetical protein	34.496	42.358	33.503	79.019	99.46	86.542	6.45E-07	-0.95681
Sant_P0204	-	hypothetical protein	54.075	50.829	45.602	183.04	156.42	93.559	2.12E-05	-0.94116

Table 3.2. (Continued)

Locus	Gene name	product	ctYpeR 3	ctYpeR 2	ctYpeR 1	ctYenR 3	ctYenR 2	ctYenR 1	padj	log2 Fold change
Sant_0812	-	Putative phage-related transmembrane protein	12.12	14.825	16.752	44.011	47.92	36.254	NA	-0.91455
Sant_3874	-	Ser/Thr protein phosphatase domain protein	43.82	40.24	31.642	76.018	92.23	83.034	1.75E-05	-0.84331
Sant_0881	-	Putative glycosidase	194.86	200.14	184.27	389.09	368	326.29	7.17E-13	-0.83279
Sant_2972	htpG	Heat shock protein HSP90	832.57	778.32	874.81	1374.3	1392	1616.2	2.08E-20	-0.78017
Sant_1243	cysK	Cysteine synthase A	64.331	70.949	74.452	108.03	137.4	153.2	1.30E-05	-0.75824
Sant_P012 6	-	Putative intracellular protease/amidase	25.173	18.002	18.613	53.013	48.83	39.763	NA	-0.75822
Sant_3551	groES	Cpn10 chaperonin GroES	1171.9	1149	1160.5	1875.5	1880	2206.8	2.38E-21	-0.74548
Sant_3402	dnaK	Molecular chaperone	1183.1	1301.4	1431.3	1991.5	2165	2553	4.62E-15	-0.73487

Table 3.2. (Continued)

Locus	Gene name	product	ctYpeR 3	ctYpeR 2	ctYpeR 1	ctYenR 3	ctYenR 2	ctYenR 1	padj	log2 Fold change
Sant_ps2409	-	-	44.752	50.829	48.394	89.021	101.27	81.865	0.00019	-0.72184
Sant_3550	groEL	Cpn60 chaperonin GroEL	5525	5699.2	5983.1	8993.2	9345.7	10433	1.30E-25	-0.71979
Sant_ps2804	-	-	9.32332	10.589	12.098	29.007	29.838	25.729	NA	-0.70818
Sant_2444	pirA	JHE-like toxin	7.45866	4.2358	7.4452	24.006	17.18	22.22	NA	-0.69293
Sant_P0291	-	hypothetical protein	5.59399	6.3537	6.5145	21.005	17.18	23.39	NA	-0.69282
Sant_1375	ompC	Outer membrane protein C	2988.13	2775.5	2867.3	4369.1	4312.1	5196.1	3.63E-17	-0.65926
Sant_3151	gmhA	Phosphoheptose isomerase	110.948	118.6	123.78	187.05	197.11	205.83	6.86E-06	-0.65246
Sant_2389	-	Lytic transglycosylase catalytic	48.4813	51.888	52.116	93.022	78.664	99.407	0.00105	-0.64567

Table 3.2. (Continued)

Locus	Gene name	product	ctYpeR 3	ctYpeR 2	ctYpeR 1	ctYenR 3	ctYenR 2	ctYenR 1	padj	log2 Fold change
Sant_2430	-	Put. LPS biosynth. glycosyltransferase	112.81	124.96	107.96	173.04	188.97	210.51	2.19E-05	-0.63705
Sant_3390	carA	Carbamoyl phosphate synthase small subunit	181.8	192.73	207.53	305.07	294.76	346.17	3.55E-07	-0.63677
Sant_1450	wcaK	Extracell. polysacch. pyruvyl transferase	148.24	132.37	136.81	217.05	230.57	229.22	6.06E-06	-0.62373
Sant_1085	grpE	Heat shock protein	278.77	273.21	289.43	409.1	428.58	491.19	4.28E-08	-0.61063
Sant_2998	lon	DNA-binding ATP-dependent protease	514.65	517.82	607.71	774.19	847.22	950.8	1.56E-09	-0.60947
Sant_1266	nupC	Nucl. transport protein	221.9	234.03	213.12	349.08	343.59	354.36	2.54E-07	-0.5992
Sant_3170	clpB	ATP-dependent chaperone protein	322.59	318.74	327.59	444.11	503.63	532.12	1.17E-07	-0.57079
Sant_0925	metN	Put. ABC transport. ATP-binding protein	169.68	144.02	139.6	228.05	230.57	243.25	5.82E-05	-0.56346

Table 3.2. (Continued)

Locus	Gene name	product	ctYpeR 3	ctYpeR 2	ctYpeR 1	ctYenR 3	ctYenR 2	ctYenR 1	padj	log2 Fold change
Sant_2116	prs	Putative ribose-phosphate pyrophosphokinase	491.34	475.46	474.63	717.17	700.74	749.65	3.70E-10	-0.56065
Sant_0719	-	DeoR family transcriptional regulator	58.737	57.183	57.7	99.024	92.227	88.881	0.005286	-0.55314
Sant_1334	ackA	Acetate kinase (Acetokinase)	961.23	972.11	911.11	1356.3	1333.7	1537.9	2.48E-11	-0.54862
Sant_1707	ftnA	Ferritin	21.444	12.707	17.682	36.009	29.838	35.085	NA	-0.54471
Sant_1921	-	hypothetical protein	216.3	189.55	211.26	290.07	311.94	326.29	1.83E-05	-0.53729
Sant_2100	nadE	NH(3)-dependent NAD(+) synthetase	118.41	109.07	107.96	180.04	161.85	170.75	0.000698	-0.53366
Sant_1928	fnr	Fumarate/nitrate reduction transcriptional regulator	229.35	245.67	214.05	339.08	349.02	335.64	8.54E-06	-0.53087
Sant_0091	ibpB	Heat shock protein B	67.128	57.183	67.007	101.02	98.556	101.75	0.006981	-0.52842

Table 3.2. (Continued)

Locus	Gene name	product	ctYpeR 3	ctYpeR 2	ctYpeR 1	ctYenR 3	ctYenR 2	ctYenR 1	padj	log2 Fold change
Sant_2492	yceA	Rhodanese domain protein	167.82	162.018	161.002	242.06	226.95	268.98	0.000132	-0.52724
Sant_1333	pta	Phosphate acetyltransferase	1557.93	1428.51	1368.05	2011.5	2066.1	2273.5	3.86E-11	-0.524189
Sant_0489	fimC1	Fimbrial chaperone protein	87.6392	95.3048	99.5794	153.04	131.11	148.53	0.002166	-0.523663
Sant_2660	artI	Arginine ABC transporter periplasmic component	238.677	223.437	221.494	309.07	341.78	362.54	1.98E-05	-0.521632
Sant_3011	yajQ	Putative nucleotide-binding protein	104.421	113.307	108.886	157.04	179.03	156.71	0.001271	-0.520234
Sant_0323	-	5-carboxymethyl-2-hydroxymuconate delta-isomerase	44.752	44.4756	39.0873	70.017	68.718	67.831	0.021079	-0.517271
Sant_2976	apt	Adenine phosphoribosyl transferase	151.97	137.662	164.725	226.05	216.1	235.07	0.00035	-0.512475
Sant_3883	pgi	Glucose-6-phosphate isomerase	423.279	419.341	377.843	538.13	622.08	617.49	9.16E-07	-0.511787

Table 3.2. (Continued)

Locus	Gene name	product	ctYpeR 3	ctYpeR 2	ctYpeR 1	ctYenR 3	ctYenR 2	ctYenR 1	padj	log2 Fold change
Sant_3766	-	Alcohol dehydrogenase GroES domain protein	87.639	109.07	132.152	153.04	151	196.47	0.004819	-0.50651
Sant_1437	sfcA	Malate dehydrogenase	194.86	176.84	183.338	288.07	245.03	284.19	0.000187	-0.50351
Sant_1419	lysP	Lysine-specific permease-associated protein	175.28	165.19	157.28	250.06	216.1	268.98	0.000439	-0.50131
Sant_2718	glnH	Cysteine ABC transporter periplasmic substrate binding protein	35.429	24.356	38.1566	52.013	45.209	67.831	NA	-0.50126
Sant_3073	dan	N-acyl-D-amino-acid deacylase	41.023	33.886	38.1566	64.015	56.964	61.983	NA	-0.5009
Sant_3639	-	2;5-diketo-D-gluconic acid reductase A	39.158	46.593	45.6018	64.015	84.993	58.475	0.032552	-0.49566
Sant_2512	ybjX	Virulence factor VirK	472.69	457.46	416	614.15	653.73	660.76	5.38E-07	-0.49241
Sant_2332	-	Anaerobic C4-dicarboxylate transporter	158.5	119.66	158.21	196.05	206.15	244.42	0.001794	-0.49142

Table 3.2. (Continued)

Locus	Gene name	product	ctYpeR 3	ctYpeR 2	ctYpeR 1	ctYenR 3	ctYenR 2	ctYenR 1	padj	log2 Fold change
Sant_0488	-	Fimbrial protein	326.32	343.1	308.98	470.113	438.53	499.37	6.79E-06	-0.49141
Sant_0195	prlC	Oligopeptidase A	320.72	312.39	343.41	428.103	462.0388	519.25	1.32E-05	-0.4912
Sant_3035	ahpC	Putative peroxidase	909.02	816.44	867.36	1169.28	1139.274	1406.9	3.18E-07	-0.491
Sant_1242	ptsH	Phosphocarrier protein	822.32	797.38	690.54	1053.25	1064.226	1177.7	1.44E-07	-0.48811
Sant_3146	gpt	Xanthine-guanine phosphoribosyl transferase	154.77	168.37	182.41	240.058	247.7468	245.59	0.000455	-0.48583
Sant_1176	thiM	Hydroxyethylthiazole kinase	50.346	48.711	62.353	81.0195	81.37669	86.542	0.024559	-0.48465
Sant_1399	efeU	Iron permease FTR1	63.399	79.421	55.839	101.024	90.41855	109.93	0.019387	-0.48322
Sant_1541	-	Hydantoinase/5-oxoprolinase	20.511	19.061	26.058	40.0096	31.64649	42.102	NA	-0.48042

Table 3.2. (Continued)

Locus	Gene name	product	ctYpeR 3	ctYpeR 2	ctYpeR 1	ctYenR 3	ctYenR 2	ctYenR 1	padj	log2 Fold change
Sant_2005	fumC	Fumarate hydratase	193.93	183.197	223.36	256.06	292.052	321.61	0.00054	-0.47961
Sant_0090	ibpA	Heat shock protein A	62.466	58.2418	85.62	90.022	97.652	128.64	0.02375	-0.47861
Sant_1983	-	hypothetical protein	33.564	31.7683	31.642	55.013	48.826	51.458	NA	-0.47291
Sant_1576	-	TonB-dependent siderophore receptor	138.92	147.193	155.42	208.05	188.975	242.09	0.00222	-0.46846
Sant_2961	ybbN	Thioredoxin domain-containing protein	131.46	135.545	164.72	189.05	204.346	230.39	0.00296	-0.46487
Sant_4066	xanP	Uracil-xanthine permease	108.15	101.658	142.39	175.04	153.712	185.95	0.00756	-0.46419
Sant_1609	-	Putative carbon-nitrogen hydrolase	110.95	99.5406	95.857	154.04	146.478	143.85	0.00726	-0.46298
Sant_2142	-	hypothetical protein	42.887	42.3577	45.602	78.019	58.7721	64.322	0.05143	-0.45954

Table 3.2. (Continued)

Locus	Gene name	product	ctYpeR 3	ctYpeR 2	ctYpeR 1	ctYenR 3	ctYenR 2	ctYenR 1	padj	log2 Fold change
Sant_2980	acrA2	Acriflavin efflux protein	592.96	655.49	621.67	815.197	859.88	930.92	7.92E-07	-0.45683
Sant_1613	-	Transcriptional regulator; LacI family	25.173	24.356	29.781	39.0094	44.305	45.61	NA	-0.45648
Sant_1016	-	hypothetical protein	296.48	276.38	267.1	434.105	349.02	398.8	0.00024	-0.45376
Sant_1824	xthA	Exodeoxyribonuclease III	108.15	97.423	115.4	149.036	147.38	167.24	0.008236	-0.45369
Sant_2614	aspC	Aromatic amino acid aminotransferase	471.76	481.82	422.51	622.15	662.77	625.68	5.70E-06	-0.4513
Sant_1209	gcvR	Glycine cleavage system transcriptional repressor	58.737	48.711	46.532	88.0212	61.485	84.204	0.051045	-0.45079
Sant_0557	-	D-isomer specific 2-hydroxyacid dehydrogenase NAD-binding; inverted	33.564	29.65	36.295	44.0106	63.293	47.949	NA	-0.44431
Sant_2522	-	hypothetical protein	41.955	46.593	48.394	65.0157	70.526	70.17	0.057115	-0.44397

Table 3.2. (Continued)

Locus	Gene name	product	ctYpeR 3	ctYpeR 2	ctYpeR 1	ctYenR 3	ctYenR 2	ctYenR 1	padj	log2 Fold change
Sant_3949	trmA	TRNA (uracil-5-)-methyltransferase	150.106	140.84	122.85	175.04	216.1	194.14	0.0061	-0.443067
Sant_2912	-	Putative phage repressor CI	14.9173	14.825	14.89	23.006	27.126	29.237	NA	-0.441437
Sant_3852	fcuA	TonB-dependent siderophore receptor	325.384	309.21	329.45	432.1	415.93	492.36	0.00012	-0.440526
Sant_2674	dacC	D-alanyl-D-alanine carboxypeptidase; Penicillin binding protein	147.309	144.02	126.57	194.05	186.26	209.34	0.00492	-0.439417
Sant_3401	dnaJ	Chaperone protein	254.527	270.03	307.11	321.08	392.42	451.42	0.00166	-0.438419
Sant_2234	-	LacI family transcriptional repressor	30.767	32.827	26.058	47.011	47.018	45.61	NA	-0.436012
Sant_1180	-	Protease/peptidase U32	170.617	148.25	122.85	197.05	202.54	223.37	0.00706	-0.435543
Sant_3969	hslV	ATP-dependent protease subunit	117.474	110.13	104.23	135.03	152.81	184.78	0.01588	-0.433156

Table 3.2. (Continued)

Locus	Gene name	product	ctYpeR 3	ctYpeR 2	ctYpeR 1	ctYenR 3	ctYenR 2	ctYenR 1	padj	log2 Fold change
Sant_1645	-	hypothetical protein	53.143	58.242	56.7696	81.02	77.76	87.712	0.0502	-0.432591
Sant_3072	-	Alanine racemase domain-containing protein	123.07	87.892	101.441	135.03	149.19	161.39	0.0195	-0.430702
Sant_2540	-	Tail sheath protein	19.579	20.12	18.613	33.008	31.646	31.576	NA	-0.427656

Table 3.3. Pairwise log-rank tests on weevil survival.

Strain 1[(1)]	Strain 2	X^2	Df[(2)]	P-value	Significance[(3)]
Δ*ypeI*	Δ*ypeR*Δ*yenR*	4.02	1	0.045	
Δ*ypeI*	Δ*ypeR*	127.0	1	1.7e-29	**
Δ*ypeI*	Δ*yenR*	196.0	1	1.5e-44	**
Δ*ypeI*	WT	231.0	1	3.9e-52	**
Δ*ypeR*Δ*yenR*	Δ*ypeR*	90.6	1	1.8e-21	**
Δ*ypeR*Δ*yenR*	Δ*yenR*	135.0	1	3.3e-31	**
Δ*ypeR*Δ*yenR*	WT	151.0	1	1.3e-34	**
Δ*ypeR*	Δ*yenR*	19.5	1	1.0e-05	**
Δ*ypeR*	WT	133.0	1	8.1e-31	**
Δ*yenR*	WT	92.1	1	8.1e-22	**
WT	Δ*ypeI-1* + WT	3.2	1	0.074	
WT	Δ*ypeR* + WT	104.0	1	2.3e-24	**
WT	Δ*ypeI-1*	192.0	1	1.1e-43	**
Δ*ypeI-1* + WT	Δ*ypeR* + WT	34.7	1	3.7e-09	**
Δ*ypeI-1* + WT	Δ*ypeR*	51.0	1	9.1e-13	**
Δ*ypeI-1* + WT	Δ*ypeI*	112.0	1	4.1e-26	**
Δ*ypeR* + WT	Δ*ypeR*	2.16	1	0.14	
Δ*ypeR* + WT	Δ*ypeI*	54.1	1	1.9e-13	**
Δ*ypeR*	Δ*ypeI*	90.8	1	1.6e-21	**
WT	Δ*cpmAJ*	0.015	1	0.9	
WT	Δ*ypeI* Δ*pirA*	147.0	1	9.3e-34	**
WT	Δ*ypeI* Δ*pirB*	170.0	1	5.8e-39	**
WT	Δ*ypeI* Δ*regC*	147.0	1	8.7e-34	**
WT	Δ*ypeI* Δ*cpmAJ*	227.0	1	2.7e-51	**
Δ*cpmAJ*	Δ*ypeI* Δ*pirA*	158.0	1	2.7e-36	**
Δ*cpmAJ*	Δ*ypeI* Δ*pirB*	191.0	1	2.1e-43	**
Δ*cpmAJ*	Δ*ypeI* Δ*regC*	162.0	1	3.6e-37	**
Δ*cpmAJ*	Δ*ypeI*	230.0	1	5.2e-52	**
Δ*cpmAJ*	Δ*ypeI* Δ*cpmAJ*	226.0	1	4.2e-51	**
Δ*ypeI* Δ*pirA*	Δ*ypeI* Δ*pirB*	3.0	1	0.083	
Δ*ypeI* Δ*pirA*	Δ*ypeI* Δ*regC*	1.33	1	0.25	
Δ*ypeI* Δ*pirA*	Δ*ypeI*	105.0	1	1.3e-24	**
Δ*ypeI* Δ*pirA*	Δ*ypeI* Δ*cpmAJ*	97.7	1	4.9e-23	**
Δ*ypeI* Δ*pirB*	Δ*ypeI* Δ*regC*	0.229	1	0.63	

Table 3.3. (Continued)

Strain 1[(1)]	Strain 2	X^2	Df[(2)]	P-value	Significance[(3)]
Δ*ypeI* Δ*pirB*	Δ*ypeI*	222.0	1	3.2e-50	**
Δ*ypeI* Δ*regC*	Δ*ypeI*	145.0	1	2.6e-33	**
Δ*ypeI* Δ*regC*	Δ*ypeI* Δ*cpmAJ*	134.0	1	5.0e-31	**
Δ*ypeI*	Δ*ypeI* Δ*cpmAJ*	0.399	1	0.53	
Δ*ypeR*	Δ*ypeI* Δ*pirA*	1.42	1	0.23	
Δ*ypeR*	Δ*ypeI* Δ*pirB*	0.112	1	0.74	
Δ*ypeR*	Δ*ypeI* Δ*regC*	0.0161	1	0.9	
WT	Δ*ypeI* Δ*pirAB*	169.0	1	1.5e-38	**
Δ*ypeI*	Δ*ypeI* Δ*pirAB*	6.73	1	0.0095	
Δ*ypeR*	Δ*ypeI* Δ*pirAB*	2.56	1	0.11	
Δ*yenR*	Δ*ypeI* Δ*pirAB*	44.6	1	2.4e-11	**
Δ*ypeR*Δ*yenR*	Δ*ypeI* Δ*pirAB*	66.3	1	3.8e-16	**
Δ*cpmAJ*	Δ*ypeI* Δ*pirAB*	170.0	1	7.6e-39	**
Δ*ypeI* Δ*pirA*	Δ*ypeI* Δ*pirAB*	0.152	1	0.7	
Δ*ypeI* Δ*pirB*	Δ*ypeI* Δ*pirAB*	4.94	1	0.026	
Δ*ypeI* Δ*regC*	Δ*ypeI* Δ*pirAB*	2.54	1	0.11	
Δ*ypeI* Δ*cpmAJ*	Δ*ypeI* Δ*pirAB*	89.7	1	2.8e-21	**
Δ*ypeI*Δ*pirAB* Δ*regC*	Δ*ypeI* Δ*pirAB*	13.1	1	0.00029	**
WT + Δ*ypeI-1*	Δ*ypeI* Δ*pirAB*	66.4	1	3.7e-16	**
WT + Δ*yenR*	Δ*ypeI* Δ*pirAB*	20.9	1	4.9e-06	**
WT + Δ*ypeR*	Δ*ypeI* Δ*pirAB*	8.52	1	0.0035	**
WT	Δ*ypeI* Δ*pirAB* Δ*regC*	91.6	1	1.1e-21	**
Δ*ypeI*	Δ*ypeI* Δ*pirAB* Δ*regC*	95.8	1	1.3e-22	**
Δ*ypeR*	Δ*ypeI* Δ*pirAB* Δ*regC*	5.08	1	0.024	
Δ*yenR*	Δ*ypeI* Δ*pirAB* Δ*regC*	8.38	1	0.0038	**
Δ*ypeR*Δ*yenR*	Δ*ypeI* Δ*pirAB* Δ*regC*	55.0	1	1.2e-13	**
Δ*cpmAJ*	Δ*ypeI* Δ*pirAB* Δ*regC*	98.2	1	3.8e-23	**
Δ*ypeI* Δ*pirA*	Δ*ypeI* Δ*pirAB* Δ*regC*	10.2	1	0.0014	**
Δ*ypeI* Δ*pirB*	Δ*ypeI* Δ*pirAB* Δ*regC*	3.46	1	0.063	
Δ*ypeI* Δ*regC*	Δ*ypeI* Δ*pirAB* Δ*regC*	3.98	1	0.046	
Δ*ypeI* Δ*cpmAJ*	Δ*ypeI* Δ*pirAB* Δ*regC*	93.7	1	3.7e-22	**
WT + Δ*ypeI-1*	Δ*ypeI* Δ*pirAB* Δ*regC*	33.7	1	6.4e-09	**
WT + Δ*yenR*	Δ*ypeI* Δ*pirAB* Δ*regC*	5.4	1	0.02	
WT + Δ*ypeR*	Δ*ypeI* Δ*pirAB* Δ*regC*	0.0096	1	0.92	
WT	WT + Δ*yenR*	47.5	1	5.5e-12	**

Table 3.3. (Continued)					
Strain 1[(1)]	**Strain 2**	**X^2**	**Df[(2)]**	**P-value**	**Significance[(3)]**
Δ*ypeI*	WT + Δ*yenR*	57.5	1	3.4e-14	**
Δ*ypeR*	WT + Δ*yenR*	11.9	1	0.00057	**
Δ*yenR*	WT + Δ*yenR*	0.0745	1	0.78	
Δ*ypeR*Δ*yenR*	WT + Δ*yenR*	54.0	1	2.0e-13	**
Δ*cpmAJ*	WT + Δ*yenR*	46.9	1	7.6e-12	**
Δ*ypeI* Δ*pirA*	WT + Δ*yenR*	16.4	1	5.2e-05	**
Δ*ypeI* Δ*pirB*	WT + Δ*yenR*	13.2	1	0.00028	**
Δ*ypeI* Δ*regC*	WT + Δ*yenR*	11.9	1	0.00056	**
Δ*ypeI* Δ*cpmAJ*	WT + Δ*yenR*	87.3	1	9.4e-21	**
WT + Δ*ypeI-1*	WT + Δ*yenR*	13.3	1	0.00027	**
WT + Δ*ypeR*	WT + Δ*yenR*	4.22	1	0.04	
Δ*ypeI* Δ*pirB*	Δ*ypeI* Δ*cpmAJ*	210.0	1	1.4e-47	**

[1] Δ*ypeI* indicates the Δ*ypeI::Spc* allele, Δ*ypeI-1* indicates the Δ*ypeI::Kan* allele.
[2] df: degrees of freedom.[3] ** indicates p-value < 0.01, of pairwise log-rank tests

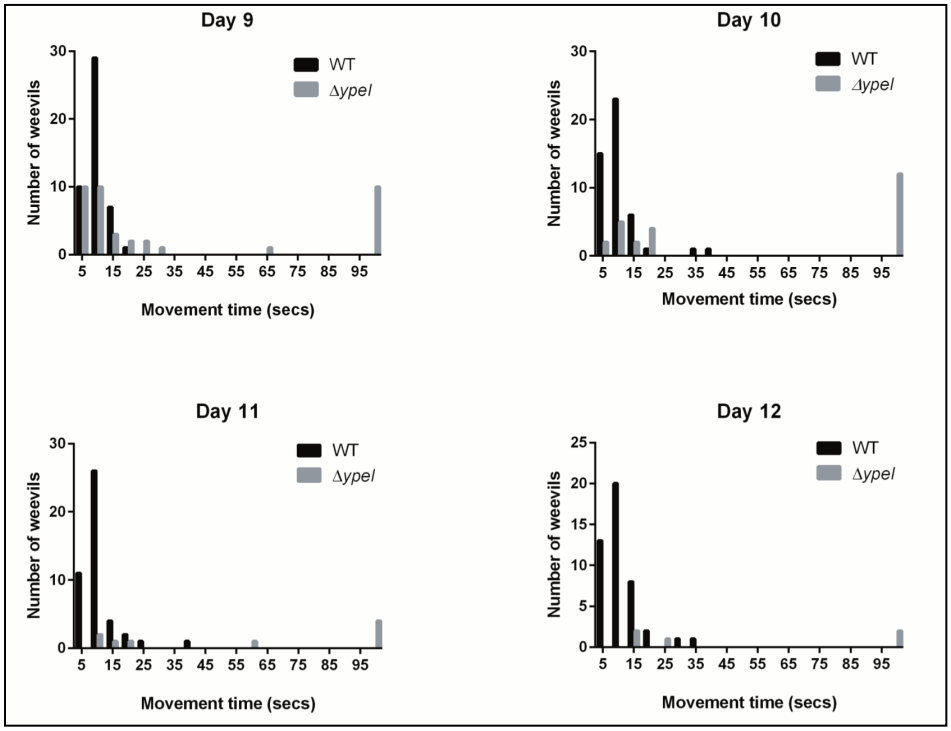

Figure 3.3. Weevil movement following injection of *S. praecaptivus* WT and Δ*ypeI* strains. Histograms depict the average time taken by a group of weevils to complete a movement assay, on days 9, 10, 11 and 12 following injection with WT and Δ*ypeI* strains of *S. praecaptivus*. Any weevils that could not complete the movement assay within the total observation time of 100 seconds were binned into the >95 second category.

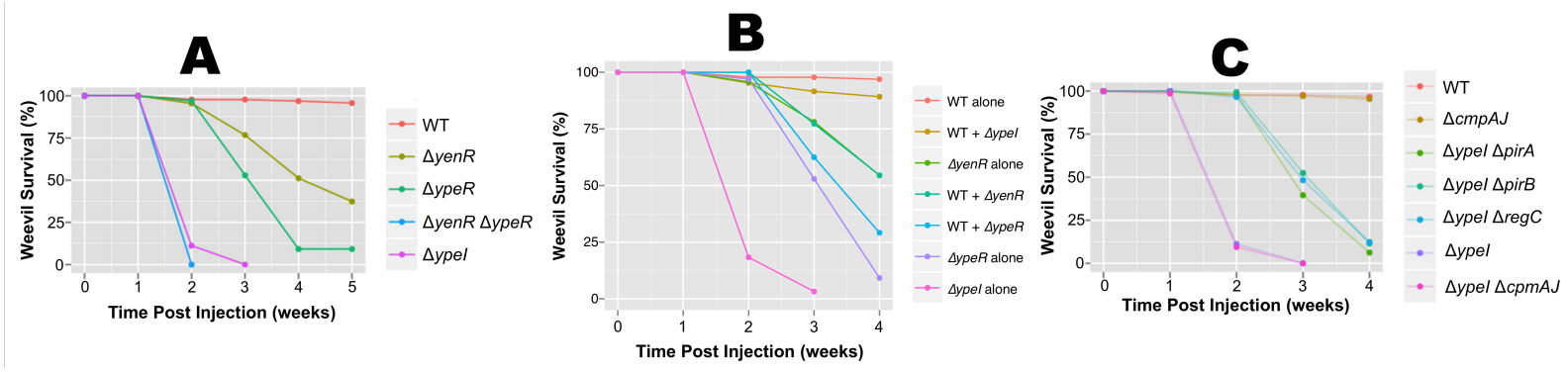

Figure 3.4. Weevil survival following injection of WT and mutant *S. praecaptivus*
(A) Inactivation of genes involved in the *S. praecaptivus* QS system results in weevil killing. Note that the "+" symbol indicates injection of equal numbers of the WT and respective mutant strain. The WT strain complements the killing phenotype of the Δ*ypeI* mutant strain. (B) Highlighting the role of the response regulators YpeR and YenR in weevil killing. Inactivation of both YpeR and YenR in a double mutant strain yields the most potent killing phenotype. (C) Identification of genes that mediate weevil killing. Inactivation of *pirA*, *pirB* and *regC* genes mitigates weevil killing in a Δ*ypeI* genetic background.

Table 3.4. Weevil infection experiments with *S. praecaptivus* mutant strains

***S. praecaptivus* genotype**	**Injections [1]**	**Median Lifespan (weeks)**
wild type	151	17
Δ*ypeI*::Kan	97	1.4
Δ*ypeI*::Spc	122	1.4
Δ*ypeR*::Spc	82	3.1
Δ*yenR*::Spc	156	4.1
Δ*ypeR*::Gen Δ*yenR*::Spc	33	1.4
Δ*ypeI*::Spc Δ(*agaR-agaF*)::Gen	30	1.4
Δ*ypeI*::Spc Δ*pirB*::Gen	89	3.1
Δ*ypeI*::Spc ΔSant_1963::Gen	68	1.4
Δ*ypeI*::Spc ΔSant_1090::Gen	43	1.4
Δ*ypeI*::Spc Δ*pirAB*::Gen	50	3.1
Δ*ypeI*::Spc ΔSant_2430::Gen	50	1.4
Δ*ypeI*::Spc Δ*cpmAJ*::Gen	74	1.4
Δ*ypeI*::Spc ΔSant_1984::Gen	44	1.4
Δ*ypeI*::Spc Δ*regC*::Gen	59	3.1
Δ*ypeI*::Spc ΔSant_P0288::Gen	31	1.4
Δ*ypeI*::Spc Δ*dmsA1BCD*::Gen	32	1.4
Δ*ypeI*::Spc Δ*pirA*::Gen	48	3.1
Δ*ypeI*::Spc ΔSant_2857::Gen	67	1.4

Table 3.4. (Continued)

***S. praecaptivus* genotype**	**Injections [1]**	**Median Lifespan (weeks)**
Δ*ypeI*::Spc ΔSant_P0292::Gen	39	1.4
Δ*ypeI*::Spc ΔSant_1963::Gen Δsant_1984::Kan	33	1.4
Δ*ypeI*::Spc Δsant_1962::Gen	39	1.4
Δ*ypeI*::Spc Δ*pirAB*::Gen Δ*regC*::Kan	23	3.5
Δ(*agaR-agaF*)::Gen	31	> 4
Δ*pirB*::Gen	39	> 4
ΔSant_1963::Gen	31	> 4
ΔSant_1090::Gen	34	> 4
Δ*pirAB*::Gen	31	> 4
ΔSant_2430::Gen	158	> 4
Δ*cpmAJ*::Gen	140	> 4
ΔSant_1984::Gen	25	> 4
Δ*regC*::Gen	31	> 4
ΔSant_P0288::Gen	30	> 4
Δ*dmsA1BCD*::Gen	44	> 4
Δ*pirA*::Gen	34	> 4
ΔSant_2857::Gen	32	> 4
ΔSant_P0292::Gen	64	> 4
ΔSant_1962::Gen	39	> 4
wild type + Δ*yenR*	22	4.1
wild type + Δ*ypeR*	24	3.1
wild type + Δ*ypeI*	79	> 4

[1]Number of weevils injected with the strain

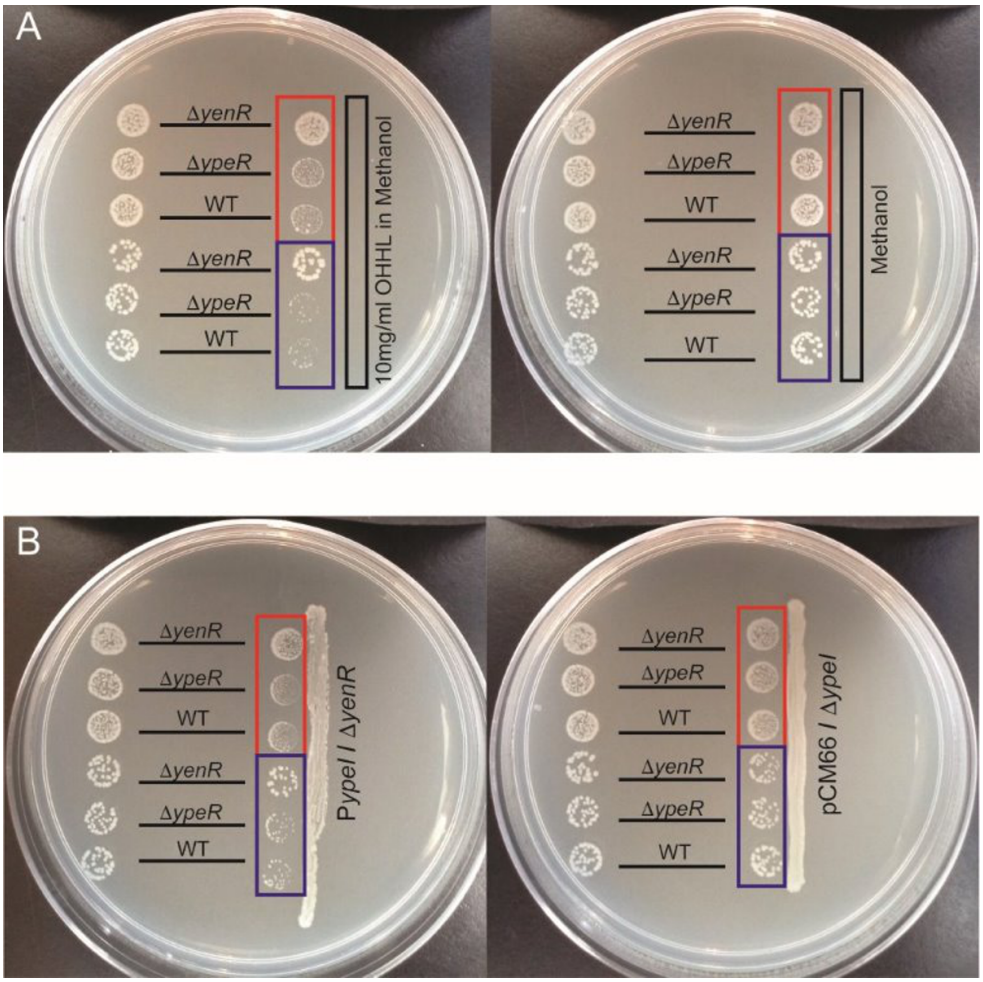

Figure 3.5. QS induces growth suppression in *S. praecaptivus*.
Each bacterial strain (label by genotype) was spotted in two positions on the plate. Panel A shows spots placed either distal (left) or proximal (right) to (A) a strip of sterile paper that was impregnated with exogenous OHHL in methanol (left plate) or methanol alone (right plate). Panel B shows spots placed either distal (left) or proximal (right) to a streak of the *S. praecaptivus* Δ*yenR* strain maintaining plasmid pCM66 overexpressing the *ypeI* gene (left plate) or a streak of the *S. praecaptivus* Δ*ypeI* strain maintaining plasmid pCM66 alone (right plate). The spots highlighted in the red boxes have a 10-fold higher concentration of cells than their counterparts highlighted in blue.

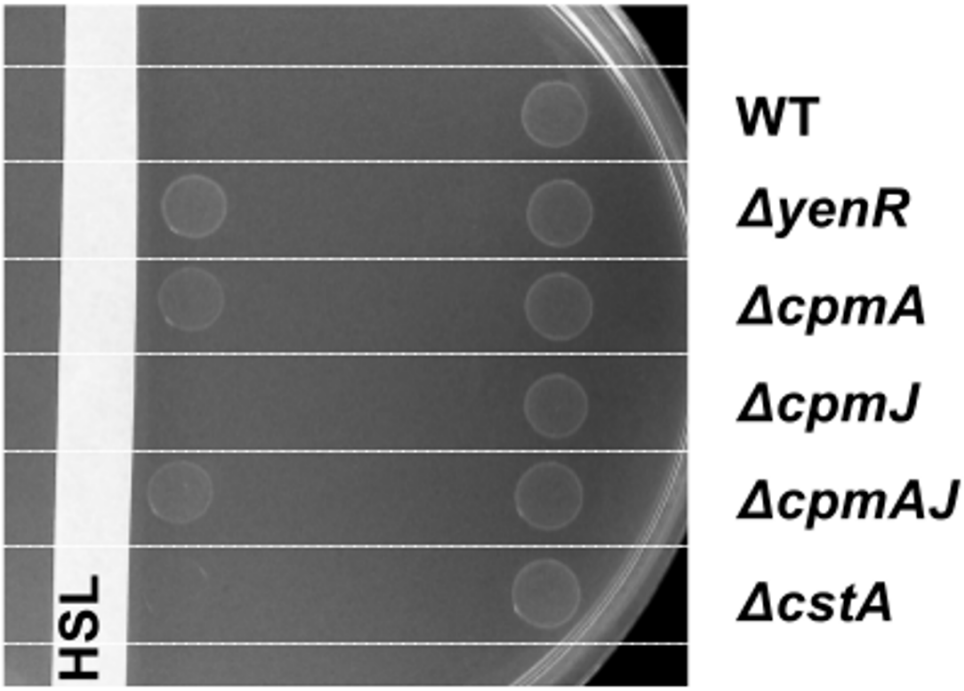

Figure 3.6. Inactivation of *cpmA* relieves growth suppression in *S. praecaptivus*.
Each bacterial strain (labeled according to genotype) was spotted in two positions on the plate, either proximal (left) or distal (right) to a strip of sterile paper that was impregnated with exogenous OHHL in methanol. Note that deletion of *cpmA* alone relieves QS-mediated growth suppression. Deletion of either *cpmJ* or *cstA* (another gene whose transcription is increased under quorum) has no effect on growth.

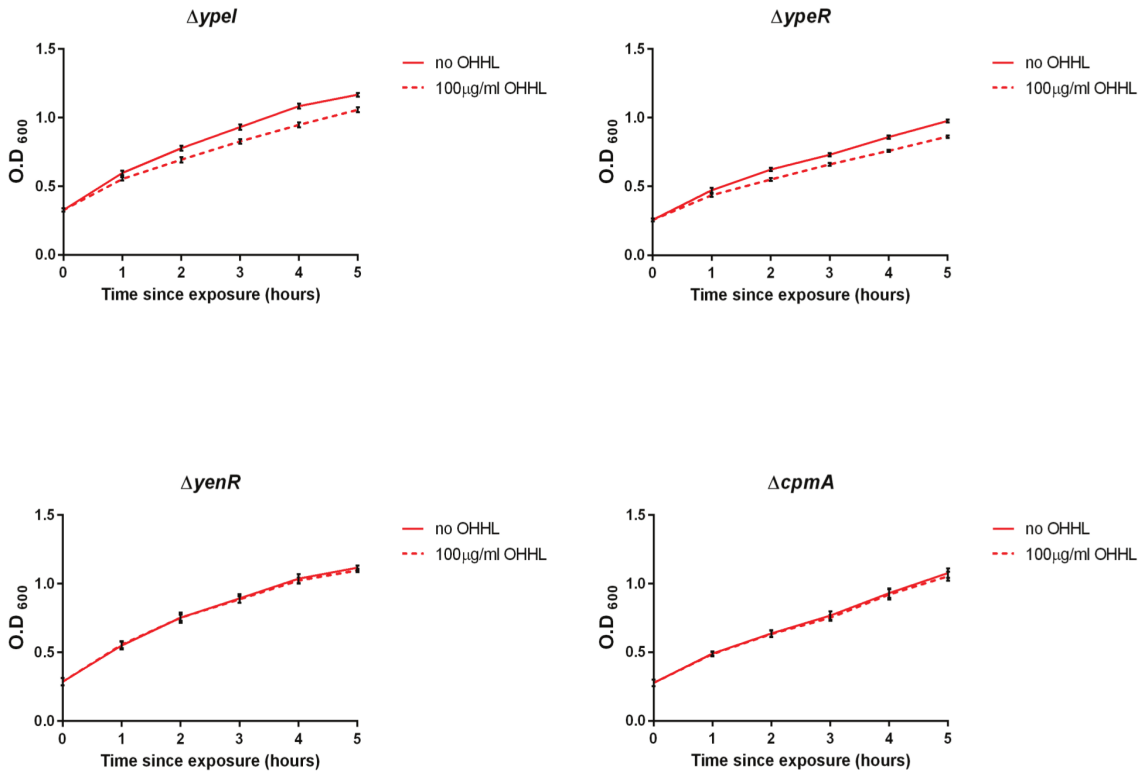

Figure 3.7. Growth curves.
Obtained from triplicate cultures of four different *S. praecaptivus* genotypes over the course of five hours in LB media at 30°C in the presence or absence of 100 μg/ml OHHL.

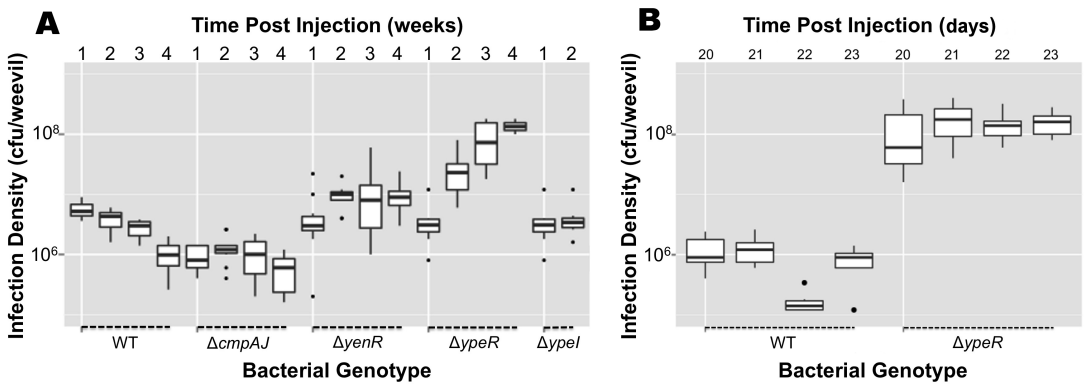

Figure 3.8. Bacterial infection densities following microinjection.
Bacterial infection densities are depicted as box plots for a range of different *S. praecaptivus* strains at various time intervals following microinjection. Note that the infection densities of the Δ*yenR* and Δ*ypeR* strains increase over time relative to the WT and Δ*cpmAJ* strains (A), particularly in the latter stages of infection, concomitant with killing (B).

3.7 References

1. Fuqua C, Parsek MR, Greenberg EP. Regulation of Gene Expression by Cell-to-Cell Communication: Acyl-Homoserine Lactone Quorum Sensing. Annu Rev Genet. 2001 Dec 1;35(1):439–68.

2. Waters CM, Bassler BL. QUORUM SENSING: Cell-to-Cell Communication in Bacteria. Annu Rev Cell Dev Biol. 2005;21(1):319–46.

3. Kievit TR de, Iglewski BH. Bacterial Quorum Sensing in Pathogenic Relationships. Infect Immun. 2000 Sep 1;68(9):4839–49.

4. Winzer K, Williams P. Quorum sensing and the regulation of virulence gene expression in pathogenic bacteria. Int J Med Microbiol. 2001;291(2):131–43.

5. Dinges MM, Orwin PM, Schlievert PM. Exotoxins of Staphylococcus aureus. Clin Microbiol Rev. 2000 Jan 1;13(1):16–34.

6. Jones S, Yu B, Bainton NJ, Birdsall M, Bycroft BW, Chhabra SR, et al. The lux autoinducer regulates the production of exoenzyme virulence determinants in Erwinia carotovora and Pseudomonas aeruginosa. EMBO J. 1993 Jun;12(6):2477–82.

7. Pirhonen M, Flego D, Heikinheimo R, Palva ET. A small diffusible signal molecule is responsible for the global control of virulence and exoenzyme production in the plant pathogen Erwinia carotovora. EMBO J. 1993 Jun;12(6):2467–76.

8. Eberhard A, Burlingame AL, Eberhard C, Kenyon GL, Nealson KH, Oppenheimer NJ. Structural identification of autoinducer of Photobacterium fischeri luciferase. Biochemistry (Mosc). 1981 Apr 1;20(9):2444–9.

9. Jones BW, Nishiguchi MK. Counterillumination in the Hawaiian bobtail squid, Euprymna scolopes Berry (Mollusca: Cephalopoda). Mar Biol. 2004 Jan 10;144(6):1151–5.

10. Boettcher KJ, Ruby EG, McFall-Ngai MJ. Bioluminescence in the symbiotic squid Euprymna scolopes is controlled by a daily biological rhythm. J Comp Physiol A. 1996;179(1):65–73.

11. Lee K-H, Ruby EG. Effect of the Squid Host on the Abundance and Distribution of Symbiotic Vibrio fischeri in Nature. Appl Environ Microbiol. 1994 May 1;60(5):1565–71.

12. Ruby EG, Asato LM. Growth and flagellation of Vibrio fischeri during initiation of the sepiolid squid light organ symbiosis. Arch Microbiol. 159(2):160–7.

13. Pontes MH, Babst M, Lochhead R, Oakeson K, Smith K, Dale C. Quorum Sensing Primes the Oxidative Stress Response in the Insect Endosymbiont, Sodalis glossinidius. Valdivia RH, editor. PLoS ONE. 2008 Oct 28;3(10):e3541.

14. Clayton AL, Oakeson KF, Gutin M, Pontes A, Dunn DM, von Niederhausern AC, et al. A Novel Human-Infection-Derived Bacterium Provides Insights into the Evolutionary Origins of Mutualistic Insect–Bacterial Symbioses. PLoS Genet. 2012;8(11):e1002990.

15. Grünwald S, Pilhofer M, Höll W. Microbial associations in gut systems of wood- and bark-inhabiting longhorned beetles [Coleoptera: Cerambycidae]. Syst Appl Microbiol. 2010 Jan;33(1):25–34.

16. Dhami MK, Buckley TR, Beggs JR, Taylor MW. Primary symbiont of the ancient scale insect family Coelostomidiidae exhibits strict cophylogenetic patterns. Symbiosis. 2013 Nov 13;61(2):77–91.

17. Fukatsu T, Koga R, Smith WA, Tanaka K, Nikoh N, Sasaki-Fukatsu K, et al. Bacterial Endosymbiont of the Slender Pigeon Louse, Columbicola columbae, Allied to Endosymbionts of Grain Weevils and Tsetse Flies. Appl Environ Microbiol. 2007 Oct 15;73(20):6660–8.

18. Koga R, Moran NA. Swapping symbionts in spittlebugs: evolutionary replacement of a reduced genome symbiont. ISME J. 2014 Jun;8(6):1237–46.

19. Arp A, Munyaneza JE, Crosslin JM, Trumble J, Bextine B. A Global Comparison of Bactericera cockerelli (Hemiptera: Triozidae) Microbial Communities. Environ Entomol. 2014 Apr 1;43(2):344–52.

20. Husnik F, McCutcheon JP. Repeated replacement of an intrabacterial symbiont in the tripartite nested mealybug symbiosis. bioRxiv. 2016 Mar 3;042267.

21. Chrudimský T, Husník F, Nováková E, Hypša V. Candidatus Sodalis melophagi sp. nov.: Phylogenetically Independent Comparative Model to the Tsetse Fly Symbiont Sodalis glossinidius. PloS One. 2012;7(7):e40354.

22. Nováková E, Hypša V. A new Sodalis lineage from bloodsucking fly Craterina melbae (Diptera, Hippoboscoidea) originated independently of the tsetse flies symbiont Sodalis glossinidius. FEMS Microbiol Lett. 2007 Apr 1;269(1):131–5.

23. Snyder AK, McMillen CM, Wallenhorst P, Rio RV. The phylogeny of Sodalis-like symbionts as reconstructed using surface-encoding loci. FEMS Microbiol Lett. 2011;317(2):143–51.

24. Kaiwa N, Hosokawa T, Kikuchi Y, Nikoh N, Meng XY, Kimura N, et al. Primary Gut Symbiont and Secondary, Sodalis-Allied Symbiont of the Scutellerid Stinkbug Cantao ocellatus. Appl Environ Microbiol. 2010 Jun 1;76(11):3486–94.

25. Kaiwa N, Hosokawa T, Kikuchi Y, Nikoh N, Meng XY, Kimura N, et al. Bacterial Symbionts of the Giant Jewel Stinkbug Eucorysses grandis (Hemiptera: Scutelleridae). Zoolog Sci. 2011 Mar 1;28(3):169–74.

26. Matsuura Y, Hosokawa T, Serracin M, Tulgetske GM, Miller TA, Fukatsu T. Bacterial Symbionts of a Devastating Coffee Plant Pest, the Stinkbug Antestiopsis thunbergii (Hemiptera: Pentatomidae). Appl Environ Microbiol. 2014 Jun 15;80(12):3769–75.

27. Hosokawa T, Kaiwa N, Matsuura Y, Kikuchi Y, Fukatsu T. Infection prevalence of Sodalis symbionts among stinkbugs. Zool Lett. 2015;1:5.

28. Oakeson KF, Gil R, Clayton AL, Dunn DM, Niederhausern AC von, Hamil C, et al. Genome Degeneration and Adaptation in a Nascent Stage of Symbiosis. Genome Biol Evol. 2014 Jan 1;6(1):76–93.

29. Waterfield N, George Kamita S, Hammock BD, Ffrench-Constant R. The Photorhabdus Pir toxins are similar to a developmentally regulated insect protein but show no juvenile hormone esterase activity. FEMS Microbiol Lett. 2005 Apr;245(1):47–52.

30. Vinetz JM, Valenzuela JG, Specht CA, Aravind L, Langer RC, Ribeiro JMC, et al. Chitinases of the Avian Malaria Parasite Plasmodium gallinaceum, a Class of Enzymes Necessary for Parasite Invasion of the Mosquito Midgut. J Biol Chem. 2000 Apr 7;275(14):10331–41.

31. Huang X, Zhao N, Zhang K. Extracellular enzymes serving as virulence factors in nematophagous fungi involved in infection of the host. Res Microbiol. 2004 Dec 1;155(10):811–6.

32. Coulthurst SJ, Barnard AML, Salmond GPC. Regulation and biosynthesis of carbapenem antibiotics in bacteria. Nat Rev Microbiol. 2005 Apr;3(4):295–306.

33. Derzelle S, Duchaud E, Kunst F, Danchin A, Bertin P. Identification, Characterization, and Regulation of a Cluster of Genes Involved in Carbapenem Biosynthesis in Photorhabdus luminescens. Appl Environ Microbiol. 2002 Aug;68(8):3780–9.

34. Miller MT, Gerratana B, Stapon A, Townsend CA, Rosenzweig AC. Crystal Structure of Carbapenam Synthetase (CarA). J Biol Chem. 2003 Oct 17;278(42):40996–1002.

35. Seibert CM, Raushel FM. Structural and catalytic diversity within the amidohydrolase superfamily. Biochemistry (Mosc). 2005 May 3;44(17):6383–91.

36. Sirikharin R, Taengchaiyaphum S, Sanguanrut P, Chi TD, Mavichak R, Proespraiwong P, et al. Characterization and PCR Detection Of Binary, Pir-Like Toxins from Vibrio parahaemolyticus Isolates that Cause Acute Hepatopancreatic Necrosis Disease (AHPND) in Shrimp. PLOS ONE. 2015 May 27;10(5):e0126987.

37. Lee C-T, Chen I-T, Yang Y-T, Ko T-P, Huang Y-T, Huang J-Y, et al. The opportunistic marine pathogen Vibrio parahaemolyticus becomes virulent by acquiring a plasmid that expresses a deadly toxin. Proc Natl Acad Sci U S A. 2015 Aug 25;112(34):10798–803.

38. Susanne B. von Bodman, W. Dietz Bauer, Coplin DL. Quorum Sensing in Plant-Pathogenic Bacteria. Annu Rev Phytopathol. 2003;41(1):455–82.

39. Ewald PW. Transmission Modes and Evolution of the Parasitism-Mutualism Continuuma. Ann N Y Acad Sci. 1987 Jul 1;503(1):295–306.

40. Elliot SL, Adler FR, Sabelis MW. How Virulent Should a Parasite Be to Its Vector? Ecology. 2003 Oct 1;84(10):2568–74.

41. Toju H, Fukatsu T. Diversity and infection prevalence of endosymbionts in natural populations of the chestnut weevil: relevance of local climate and host plants. Mol Ecol. 2011 Feb;20(4):853–68.

42. Oliver KM, Russell JA, Moran NA, Hunter MS. Facultative bacterial symbionts in aphids confer resistance to parasitic wasps. Proc Natl Acad Sci. 2003 Feb 18;100(4):1803–7.

43. Moran NA, Degnan PH, Santos SR, Dunbar HE, Ochman H. The players in a mutualistic symbiosis: Insects, bacteria, viruses, and virulence genes. Proc Natl Acad Sci U S A. 2005 Nov 22;102(47):16919–26.

44. Datsenko KA, Wanner BL. One-step inactivation of chromosomal genes in Escherichia coli K-12 using PCR products. Proc Natl Acad Sci. 2000 Jun 6;97(12):6640–5.

45. Shevchuk NA. Construction of long DNA molecules using long PCR-based fusion of several fragments simultaneously. Nucleic Acids Res. 2004 Jan 21;32(2):19e–19.

46. Zhu J, Chai Y, Zhong Z, Li S, Winans SC. Agrobacterium Bioassay Strain for Ultrasensitive Detection of N-Acylhomoserine Lactone-Type Quorum-Sensing Molecules: Detection of Autoinducers in Mesorhizobium huakuii. Appl Environ Microbiol. 2003 Nov 1;69(11):6949–53.

47. Shaw PD, Ping G, Daly SL, Cha C, Cronan JE, Rinehart KL, et al. Detecting and characterizing N-acyl-homoserine lactone signal molecules by thin-layer chromatography. Proc Natl Acad Sci. 1997 Jun 10;94(12):6036–41.

48. Price-Carter M. Beta-Galactosidase Activity Assay [Internet]. 2000 [cited 2016 Sep 20]. Available from: http://rothlab.ucdavis.edu/protocols/beta-galactosidase-3.html

49. Sung K, Khan SA, Nawaz MS, Khan AA. A simple and efficient Triton X-100 boiling and chloroform extraction method of RNA isolation from Gram-positive and Gram-negative bacteria. FEMS Microbiol Lett. 2003 Dec;229(1):97–101.

50. Patel RK, Jain M. NGS QC Toolkit: A Toolkit for Quality Control of Next Generation Sequencing Data. PLOS ONE. 2012 Feb 1;7(2):e30619.

51. Langmead B, Salzberg SL. Fast gapped-read alignment with Bowtie 2. Nat Methods. 2012 Mar 4;9(4):357–9.

52. Anders S, Pyl PT, Huber W. HTSeq—a Python framework to work with high-throughput sequencing data. Bioinformatics. 2014 Sep 25;btu638.

53. Love MI, Huber W, Anders S. Moderated estimation of fold change and dispersion for RNA-seq data with DESeq2. Genome Biol. 2014 Dec 5;15(12):1–21.

4. CONCLUSION

The work compiled in this document allows only a glimpse into the biology of *Sodalis praecaptivus*. As proposed previously, *S. praecaptivus* is likely to have served as an evolutionary precursor of the *Sodalis*-allied insect symbionts, as a proto-symbiont. The use of its OHHL quorum signal to suppress its own replication/growth appears to be a novel strategy that has not been previously encountered among other bacteria. By producing host invasion/virulence effectors when it is at a low population density, *S. praecaptivus* could infiltrate possible insect hosts. Then, having grown to a sufficient population density, it would slow down its own growth and be capable of maintaining an asymptomatic infection in the host. This would allow the host organism to retain fitness and serve as a vector to allow the transfer of *S. praecaptivus* to a wider range of hosts than would be possible with a pathogen that did not curb its virulence. The attenuation of virulence is the most important characteristic in the conversion from parasitism to mutualism, and *S. praecaptivus* shows evidence of being on just such an evolutionary trajectory. Further work is required to fully reveal all the virulence effector genes and genes repressed to produce the self-growth inhibition that *S. praecaptivus* uses, and the various levels of regulation these may be subject to.